

DEVELOPMENT OF A DIGITAL TWIN FOR
A SOLAR POWERED ELECTRIC RACE VEHICLE

by

James Bradley Baer

A thesis submitted to the faculty of
The University of North Carolina at Charlotte
in partial fulfillment of the requirements
for the degree of Master of Science in
Applied Energy and Electromechanical Engineering

Charlotte

2023

Approved by:

Dr. Maciej Noras

Dr. Michael Smith

Dr. Wesley Williams

©2023
James Bradley Baer
ALL RIGHTS RESERVED

ABSTRACT

JAMES BRADLEY BAER. Development of a Digital Twin for a Solar Powered Electric Race Vehicle. (Under the direction of DR. WESLEY WILLIAMS)

The global and local impacts of climate change have increased the interest in decarbonizing energy economies in general and transportation in particular. Solar electric vehicles (EVs) represent an intersection of renewable energy generation and EV development, both of which are topical focuses of current research in their own right. Mirroring the rise of automobiles and aviation, many of the developments in solar EVs have come from competition-based innovation.

The development of complex electromechanical systems has been assisted in recent years by the use of digital twins, which are built on physics-based models of the underlying systems. This research develops a digital twin based on a solar electric racing vehicle constructed by Appalachian State University. The digital twin consists of two interlinked models, with the first representing a 1-D model of the vehicle dynamics, electric motor, and race course. The second represents the solar panels and battery system, with the current draw on the motor linking the two models. In combination, the digital twin is driven by a variety of inputs such as motor parameters, course elevation, vehicle dimensions, battery parameters, and solar panel configuration. The key outputs from the digital twin are the vehicle speed, current draws, and SOC for the battery. The performance of the digital twin was successfully simulated on a variety of virtual tracks, starting with a flat track and constant slope course before moving to arbitrary changing slopes and imported topological data for a road course.

DEDICATION

I want to dedicate this work to my lovely wife, Madison Baer, and daughter, Elizabeth Baer, for without their love and support my pursuit of higher education would not be possible.

ACKNOWLEDGMENTS

I would like to acknowledge the help and support of Dr. Wesley Williams for the hours of troubleshooting and technical support he provided. His guidance and expertise were instrumental in the completion of my work and research.

TABLE OF CONTENTS

ABSTRACT	III
DEDICATION	IV
ACKNOWLEDGMENTS	V
LIST OF FIGURES	VIII
LIST OF ABBREVIATIONS	X
CHAPTER 1: INTRODUCTION	1
CHAPTER 2: LITERATURE REVIEW	5
2.1 ELECTRIC VEHICLES	5
2.2 SOLAR VEHICLES	12
2.3 SOLAR RACING VEHICLES	14
CHAPTER 3: DIGITAL TWINS	17
3.1 WHAT ARE DIGITAL TWINS?	17
3.2 HOW ARE DIGITAL TWINS USED IN INDUSTRY?	18
CHAPTER 4: METHODOLOGY	28
4.1 PHYSICS-BASED MODELING [SYSTEM ARCHITECTURE]	29
4.2 MOTOR MODELING	32
4.3 VEHICLE DYNAMICS MODELING	34
4.4 RACECOURSE MODELING	38
4.5 FLAT TRACK MODELING	38
4.6 ROAD COURSE MODELING	39
4.7 SOLAR PANEL MODELING	41
4.8 BATTERY MODELING	45
CHAPTER 5: RESULTS	48
5.1 TRACK SIMULATION	48
5.2 COURSE SIMULATION	52
CHAPTER 6: CONCLUSIONS AND FUTURE WORK	64
REFERENCES	71
APPENDIX A: MOTOR DATA SHEET	73
APPENDIX B: MOTOR SPECIFICATIONS	74
APPENDIX C: SOLAR CELL SPECIFICATIONS	75
APPENDIX D: BATTERY SPECIFICATIONS	76
APPENDIX E: MOTOR & DRIVE SPECIFICATIONS	77

APPENDIX F: INITIALIZATION FUNCTIONS	78
APPENDIX G: ELEVATION & DISTANCE MAPPING SOFTWARE	80
APPENDIX H: DISTANCE & GRADE RAW DATA	81
APPENDIX I: SOLAR CELL DATASHEET	86
APPENDIX J: SOLAR ARRAY DATA	88
APPENDIX K: SOLAR VEHICLE ENERGY BALANCE	89

LIST OF FIGURES

FIGURE 1: First EV Invented by Robert Anderson	5
FIGURE 2: Honda Insight	7
FIGURE 3: Tesla Charging Stations.....	9
FIGURE 4: Vehicle Dynamics Diagram	10
FIGURE 5: Electrical Diagram.....	10
FIGURE 6: Model of SC	11
FIGURE 7: William Cobb and The First Solar Powered Car.....	12
FIGURE 8: First Full Solar Vehicle	13
FIGURE 9: Basic Schematic of Solar EV System.....	14
FIGURE 10: SUNSWIFT Solar Race Car	15
FIGURE 11: Comparison of Solar Energy Produced	16
FIGURE 12: DT Growth in Research.....	18
FIGURE 13: Representation of Autodesk Digital Architecture	19
FIGURE 14: PTC Representation of DT	20
FIGURE 15: Model of a City Using 3D Experience	21
FIGURE 16: DT Representation.....	22
FIGURE 17: Cloud Integration of Big Data	23
FIGURE 18: Service Layers	24
FIGURE 19: Race Track Versus Simulation	25
FIGURE 20: Vehicle Track Trajectory.....	26
FIGURE 21: Telemetry Data Versus Real World	27
FIGURE 22: Model Capabilities	29
FIGURE 23: EV Dynamics / Motor Model.....	30
FIGURE 24: PV Solar Array /Battery Model.....	31
FIGURE 25: Motor Control and Drive	32
FIGURE 26: Motor Control Parameters	33
FIGURE 27: Longitudinal Vehicle Block	34
FIGURE 28: Vehicle Block Parameters	35
FIGURE 29: Vehicle Block with Speed Control.....	36
FIGURE 30: PI Control for Vehicle	37

FIGURE 31: Data Entry from PI	37
FIGURE 32: Road Course Model System	39
FIGURE 33: Course Grade Calculation	40
FIGURE 34: Course Grade Sub System	40
FIGURE 35: Sample Distance and Grade Value Matrix	41
FIGURE 36: Solar PV System.....	42
FIGURE 37: PV Solar Array	43
FIGURE 38: Solar PV Parameters.....	44
FIGURE 39: Solar Cell Manufacturer Datasheet	45
FIGURE 40: Battery Block System.....	46
FIGURE 41: Battery Block Parameters	47

LIST OF ABBREVIATIONS

AI	Artificial Intelligence
BMS	Business Management System
CAD	Computer Aided Drafting
CSV	Comma-separated Values
DOF	Degrees of Freedom
DT	Digital Twin
EV	Electric Vehicle
HESS	Hybrid Energy Storage System
HEV	Hybrid Electric Vehicle
HVAC	Heating Ventilation and Cooling
IoT	Internet of Things
PG	Percent Grade
PI	Proportional Integral
PV	Photovoltaic
ROSE	Racing on Solar Energy
SC	Supercapacitor
SOC	State of Charge

CHAPTER 1: INTRODUCTION

The decarbonization of the vehicle industry is pushing electric vehicle (EV) technology to the forefront of cutting-edge science and design. This surge in EV technology is forcing companies to acquire greater knowledge through cheaper and more efficient product design. Each element of an EV system presents an opportunity for improvement and is evolving to meet rising consumer demands. These systems include batteries, electrical motors, and lighter vehicle frames. The EV market expands through innovation and top quality, consumer friendly product design.

It currently costs companies millions of dollars to innovate new ways to store energy and build more efficient electric motors, which slows down innovation. For example, lithium is difficult to mine and, therefore, lithium-ion batteries are expensive to prototype and build. Solar panels are a proven way to capture energy from the sun but often require large surface areas to make them a viable power source. A new approach to product development has emerged that helps drive down innovation costs and timelines through the use of physics-based models commonly called digital twins (DT).

DT technology is an evolving industry; many businesses and research organizations are taking advantage of this technology to innovate their products or research. The leading technological Fortune 500 industries are harnessing the power of taking physical products and converting them into digital simulations. Digital models don't require huge overhead because a small development team can independently oversee the creation of a high-fidelity model, which saves on energy costs that are associated with multiple iterations of physical prototyping. As an example, when testing a cutting-edge turbine system, the number of sensors required for data acquisition alone

can cost more than the product that is being tested. With digital models, coordination with a geographically distributed team is much easier, as a model can easily be sent over the Internet as opposed to coordinating travel for scattered team members at a central testing location. The next four chapters will explore the current research that uses Simscape and Simulink to create DT simulations of EVs along with research into track ready solar powered EVs using Simscape.

Chapter 2 explores the history of the EV, how it began, and where it is heading in the future. A history of the solar EV and solar EV racing is included in this chapter to demonstrate how the EV has branched into several sub-niches that have recently exploded in popularity. Chapter 2 also contains current research into the issues EV researchers face when attempting to fill the knowledge gap. Chapter 3 shares the layout for how the DT model was created. Using Simscape block functions, a model was created to replicate the digital version of Appalachian State's solar racing EV named Racing on Solar Energy (ROSE).

Chapter 4 details the methodology for creating the DT model. The first section of methodology introduces the system architecture used in calculating battery statistics graphically. The second section explains the motor model and how it is used to simulate the real-world version located on ROSE. The third section covers vehicle dynamics. The vehicle dynamics model is the foundation of the simulation. The fourth section discusses racecourse modeling and how it will impact the output results of the EV. The fifth section covers the solar cell array power system. The solar cell system displays the advantage of adding solar cells to an EV. The final section goes over the battery, the battery and solar

cell model are the top layer of the foundational vehicle model. Both models work in unison to deliver the desired outputs.

Chapter 5 discusses the results that were obtained from the solar EV model. The results are divided into two separate sections; the first of which modeled the system on a flat track- this was done to show differences in solar current or battery charge without the external influence of varying grade levels. The second section of the results is the course track, which includes real-time road grade levels that simulate a live track. Examples of the DT's typical outputs provide graphical data on the performance of the solar race vehicle's outputs; this includes the battery voltage and charge levels, and the vehicle's velocity and position. The model outputs are dependent upon the specific profile of the course; these outputs will help identify system (battery, panel, motor, etc.) improvements and strategies for improved performance in different terrains.

Chapter 6 concludes the research and discusses the model's capabilities and limitations. The main goal of this research is to create a DT that simulates a solar racing EV to obtain a better understanding of how the vehicle operates under certain conditions. This will ultimately provide the student-led race team at Appalachian State with additional engineering insights during the development of their next-generation solar EV. The concluded work will help the team identify the weaknesses in the solar race vehicle and how to fine-tune the electrical/mechanical components to increase performance and efficiency.

Chapter 6 also touches on future work and where the current model needs refinement and how it can be improved. Several issues arose when trying to have a solar model, a battery model, and a vehicle model all on the same simulation file. As each

model represents a different domain in physics, this can cause issues for the solver when trying to run everything simultaneously. Although the current model reports reasonable values for vehicle performance, numerous refinements can be made to increase the accuracy of the model. Validation of the model against actual data obtained by ROSE would also be needed to refine the simulations and provide the user with a DT to predict solar EV racing performance based on varying track conditions at high fidelity.

CHAPTER 2: LITERATURE REVIEW

Research into the solar EV racing industry has shown that, although the industry appears to be new, aspects of the technology have been around for over a century. Due to challenging competition with petrol vehicles, the EV industry struggled to take off; however, like most of the world's largest industries, where there is demand there is innovation. The literature review touches on the history and evolution of the EV which preceded the development of solar racing EVs. Several topics are discussed that shine a light on the current challenges facing solar EVs. These topics include solar absorption rates in cities versus the open country, new ways to store more energy within battery packs, and more efficient ways to monitor state of charge (SOC) levels within a battery.

2.1 Electric Vehicles

EVs may seem new and modern but they have been around for over 100 years. Robert Anderson, a Scottish inventor, was credited for the development of the first EV, shown in Figure 1, in the late 1800s.



FIGURE 1: First EV Invented by Robert Anderson [1]

After Anderson's EV was released, a U.S. inventor named William Morrison developed a six-passenger electric carriage that ran at a top speed of 14 miles per hour [1]. Significant interest was put into the development of EVs, which continued until the turn of the 20th century. Automobile inventor Henry Ford developed the first commercial combustion engine automobile called the Model T in 1908 [1]. In the early 1900s, gas was cheap which created a high demand for combustion engines compared to the alternative, electric. Electric components were more expensive than gas powered engines, therefore, the market naturally favored the combustion engine as the industry standard and EVs fell off the map for a few decades.

In the early 1990s, the Department of Energy began research into battery technology that would allow the EV to travel long distances before needing a charge. Before our current battery technology was invented, the longest traveling EV lasted approximately 40 miles. Environmental regulations in California also contributed to cracking down on gas emissions that led to changes in the EV market [1]. The transition from petrol to electric was not clear-cut; a combination of both gas and electric-powered cars came onto the scene before any pure EV did. In 1999 Honda released a hybrid electric vehicle (HEV) called Insight shown in Figure 2. This was the first commercially successful HEV vehicle that gained a following from car lovers [2].



FIGURE 2: Honda Insight [2]

The second and most well-known HEV was the Toyota Prius and, like the Honda Insight, the first-generation Prius used a nickel metal hydride battery that allowed the HEV industry to become profitable [2]. In 2008 Tesla Motors took the electric car industry by storm by producing the Tesla Roadster EV. The Roadster was an all-electric vehicle that could run up to 245 miles on a single charge and reached a top speed of 125 mph which was quick enough to compete with most sports cars [3]. The key to the long drive time was Tesla's innovation in battery technology, as the Tesla vehicles used the lithium-ion battery instead of the nickel metal hydride. The lithium battery allowed the car to be charged from any outlet and kept the charge longer than other batteries on the market.

Today, the electric car industry's future looks bright when considering the rising gas prices and the amount of pollution coming from petrol engines. The current political climate is also shifting to greener energy which gives more grants and government money to researchers in the EV field. As charging stations and infrastructures improve for the EV industry, the cheaper the entry price will become for the consumer, which will ultimately lead to the demise of the petrol engine industry. The progression of the EV industry depends on several additional key innovations, such as battery technology. The current lithium-ion battery requires intense mining that has an impact on the environment. Lithium mining creates large craters and requires large machinery to dig and transport lithium-enriched soil enriched. Charge time from charge stations must also be considered. Figure 3 shows a photo from Energysage.com of a Nema14-50 charger for a Tesla model EV that plugs into a 240 V wall outlet and takes an average of 10 hours to charge [4]. As one can imagine, 10 hours would be a large hindrance if a driver's battery died on the way home from a trip or a long work commute. What if there was not a charging station close by? As of today, the infrastructure for long distance travel is missing, and although more and more Tesla charging stations are popping up, there is still a large gap to be filled before EVs can dominate the market.



FIGURE 3: Tesla Charging Stations [5]

Current research into EV software needs several improvements in battery technology and monitoring. A big part of simulating the electrical landscape is the ability to model and monitor real-time battery efficiency from SOC. Error free SOC is paramount in this industry when accuracy matters most for digital models [6]. Simulink by MATLAB has provided a foundation not just for battery improvements in EVs but also for vehicle dynamics in general. Figure 4 shows a general Simulink block diagram model of a petrol engine vehicle. The model incorporates several elements such as vehicle dynamics, tire dynamics, and gearcase outputs along with front and rear differential outputs. Figure 5 shows an example of an electrical model that controls a DC motor by implementing a PWM and an H-Bridge. Figure 4 and Figure 5 display how Simscape can build basic mechanical and electrical systems using physical blocks that can easily be pulled from *a list of default programs or customized to meet a specific need.*

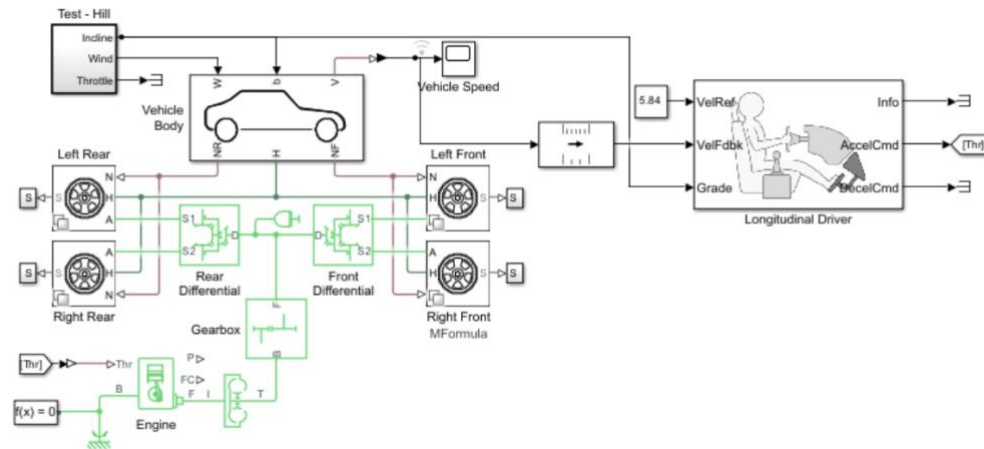


FIGURE 4: Vehicle Dynamics Diagram [7]

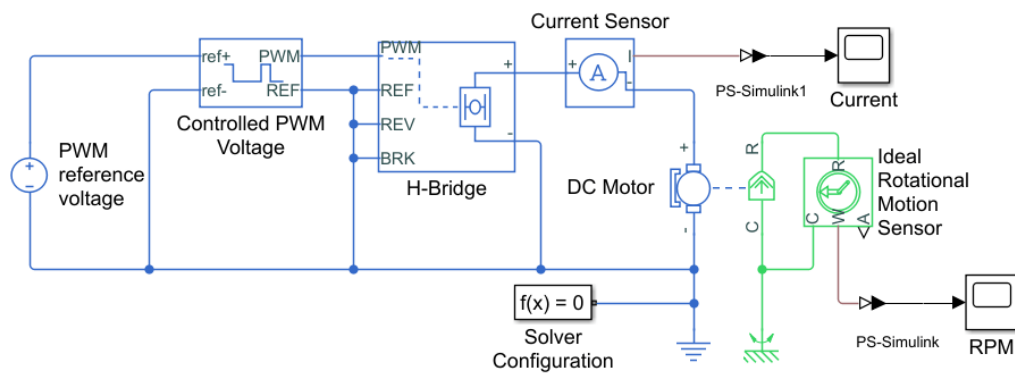


FIGURE 5: Electrical Diagram [7]

Simscape is a capable tool for DT research and meets several requirements that are needed to develop a successful model. A system-level simulation should check off four points of interest. First, the simulation needs to provide a common framework that can communicate between a systems engineer and a design engineer. Second, it needs to support behavioral system definition by defining how main components communicate with subcomponents. Third, the software needs to provide off-the-shelf functionality to eliminate the time required to create a model from scratch. Lastly, the software needs to

be customizable for the end user, this is by far the most important as every DT iteration might change [8].

Current academic research in the EV field varies greatly depending on the sector of interest. One example of current EV research is the supercapacitor (SC) technology research being performed by Canmet Energy Research Center. Here, the introduction of a SC can improve the functionality of the EV electrical system by allowing a larger capacity of energy storage, quick discharge, and extended battery life. Figure 6 shown below is a Simulink digital model of a hybrid energy storage system (HESS)/SC [9]. This model takes advantage of model subsystems; this leads to cleaner code and a better way to visualize the system. Each subsystem can easily be viewed by clicking on the sub model. The sub models can be viewed in Figure 6 as light gray boxes.

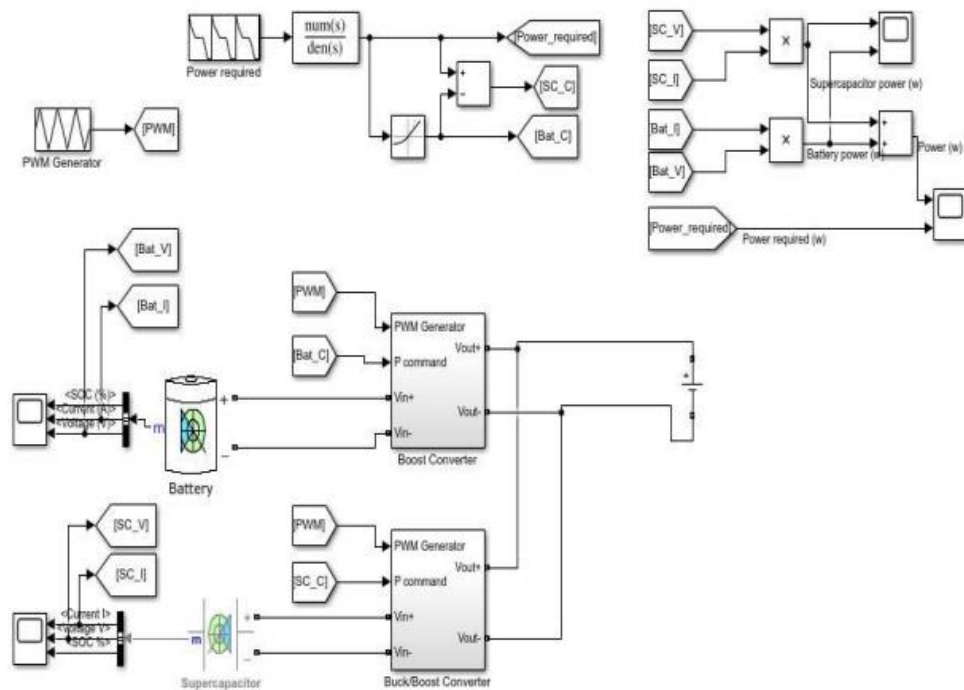


FIGURE 6: Model of SC [9]

2.2 Solar Vehicles

The first solar vehicle was invented by William G. Cobb who worked for General Motors. Cobb's invention, dubbed "The Sun Mobile", was a solar powered vehicle that had a 15-inch photovoltaic (PV) panel attached to the roof of the car [10]. The 15-inch panel shown in Figure 7 was made from close to 11,000 individual solar cells, the combined charge propelled the car using a small electric motor.



FIGURE 7: William Cobb and The First Solar Powered Car [10]

In 1980 at the engineering department of Tel Aviv Israel, a solar powered car was created that used eight batteries to store electrical energy. As seen in Figure 8, this was one of the first fully rechargeable solar powered vehicles that are in public record. The engineering department stated that the solar EV could reach 40 mph and a max range of 50 miles.



FIGURE 8: First Full Solar Vehicle [11]

Solar powered vehicles in their most basic functionality consist of a PV solar board mounted to the top or sides of a vehicle, a battery to store generated power, a DC motor, and an AC motor. The current from the solar cell is sent directly to a DC or AC motor. Solar EVs can become very complex when controllers are involved. Most performance or racing solar EVs require complicated software and subsystems to reach max output speeds and distance. An example of a basic solar cell model is shown in Figure 9. This model contains a solar unit, a battery system, several converters, and a maximum power point tracker (MPPT) that regulates the voltage coming from the solar cell. The battery system then sends current directly to the electric motor(s) on the vehicle. Solar models can be simulated in Simscape or Simulink. Both software can be used to predict the behavior of power or energetic characteristics of solar cells.

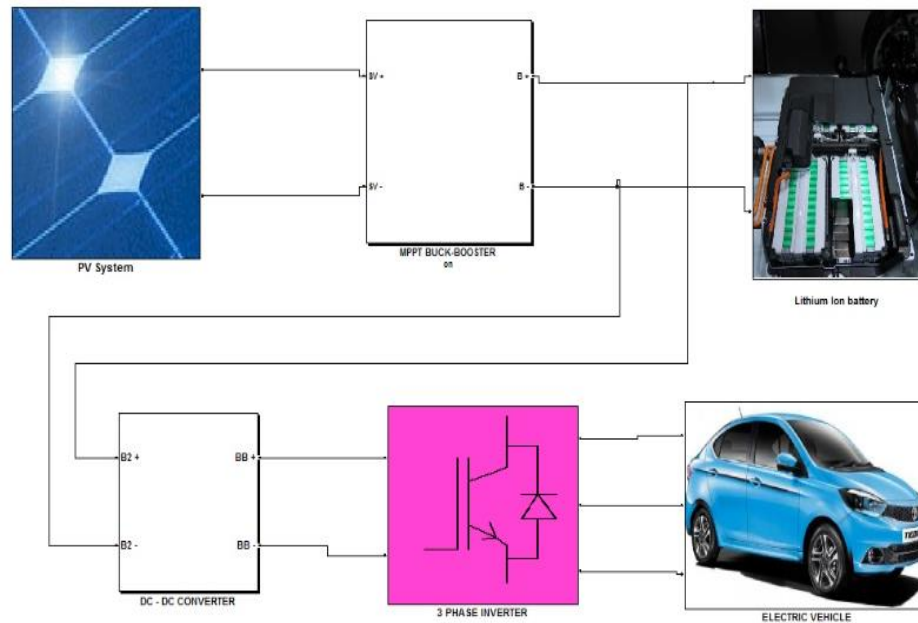


FIGURE 9: Basic Schematic of Solar EV System[12]

2.3 Solar Racing Vehicles

Beginning in 1983, Hans Tholstrup and Larry Perkins created the first solar race car, The Quiet Achiever, also known as BP Solar Trek. As shown in Figure 10, the EV was made entirely out of fiberglass and was powered solely by solar energy. The solar power system contained two rows of 10 36-cell solar panels which were rated at 1 kilowatt and could achieve an average speed of 14 mph [13]. The Quiet Achiever was able to drive up to 2500 miles in under 20 days. Following the success of The Quiet Achiever, public awareness was raised to increase competitiveness between different manufacturers and student organizations. In 1987 the Australian World Solar Challenge was the first among many to host a solar racing race. The race consisted of 23 different solar EVs. Today the world solar challenge still reigns as the top competitive solar race car event.

Solar racing is still an academic pastime, schools across the world still compete to see who can build the fastest long-lasting solar EV. The largest known American solar racing competition is The American Solar Challenge. The solar racing teams strive to travel 1975 miles over eight days while minimizing their reliance on external charging (beyond solar). Other race competitions are strictly set on a race track such as the Formula Solar Grand Prix, which is an annual solar race that is confined to a closed loop and serves as a qualifier for the American Solar Challenge.

Currently, the University of New South Wales (UNSW) has claimed the world record for the fastest solar powered vehicle. The Sunswift solar race vehicle can reach a top speed of 55.077 mph [14]. The body is constructed out of carbon fiber to reduce weight, the motor that powers the three-wheel EV is CSIRO 3 phase DC 1800 W and has a solar array producing around 1200 W of power.



FIGURE 10: SUNSWIFT Solar Race Car [14]

As of 2022, research in solar racing technology is being tested by Siam Technology College to see how the efficiency of solar EVs reacts to weather conditions and urban environments. The experiment began in Thailand with tall buildings to see if

city structures would block sun exposure to the cells. The results were compared with the open country of Australia where open land does not impede the sun's direct influence on solar cells. Figure 11 displays the results of the electrical energy produced by the solar cells [15] and shows the clear impact of the urban environment reducing the power produced by equivalent solar panels.

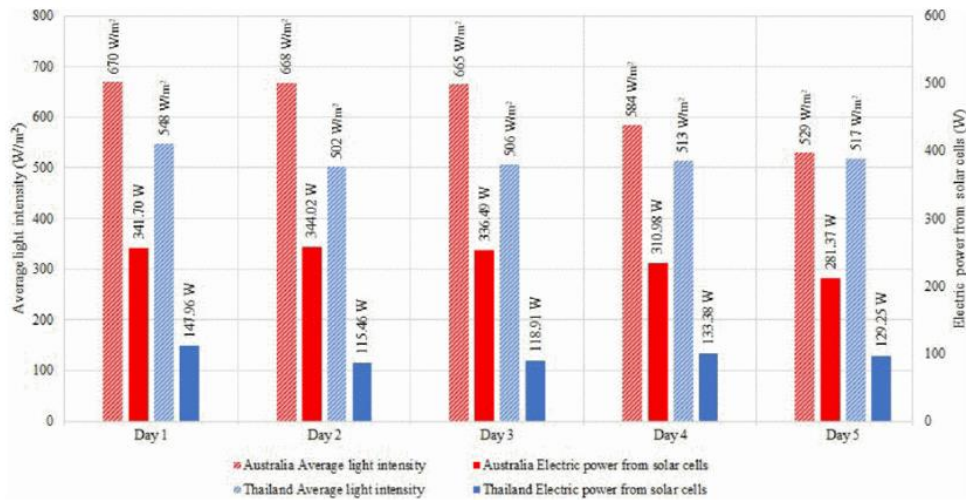


FIGURE 11: Comparison of Solar Energy Produced [15]

CHAPTER 3: DIGITAL TWINS

3.1 What are Digital Twins?

A DT can best be described as a digital model of a real-life physical object. The real-life object will typically have sensors to monitor the physical properties to convert it into digital data. Most DTs are based on mechanical designs to give feedback to the designer so that improvements can be made. Take the engine of a car for example, a current engine will typically house several sensors to track the performance of the engine or alert the driver if a mechanical failure happens. This direct feedback from a physical system allows real-time data to be monitored to create a positive feedback loop.

A DT's primary function is to allow the designer to predict how the product will respond to future use. By taking real-life parameters and creating a digital model, designers/engineers can run the model on many different scenarios to see where the model might fail. This type of predictive engineering is an attractive option for companies that want to evolve their products while keeping costs low. For some products, the cost of testing might prevent a company from making their products better; for example, the turbine company Siemens is known for testing and gathering data on new turbine engines, this can be very costly and almost impossible without infrastructure and partnerships with local energy providers. That data must come from sensors which have to come from a real-life turbine setup, a typical turbine setup is more than just a turbine, it includes piping, foundational support, generators, substation- to handle the electricity- and filtration units that are sometimes larger than the turbine itself. Once you build one setup and gather all the data, a DT can be made that will allow changes to the turbine system to improve performance without having to build a new version.

DT offer a wide range of benefits, not only do they allow for physical models to be represented in 3D, but they replicate the physics of the model. 3D models that replicate physical objects are helpful for companies that produce complicated parts and need to train new engineers on how the components mate. Companies that digitize their products in 3D will have better training material when the time comes to design or improve their products. DT research is becoming an ever-increasing topic for researchers. Figure 12 is a graph showing the growth of search results within IEEE EXPLORE. The increase in growth shows that the interest in this field grows every year.

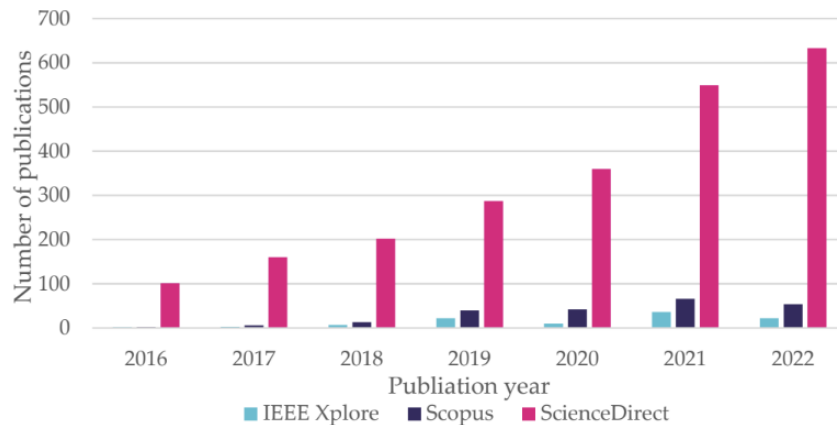


FIGURE 12: DT Growth in Research [19]

3.2 How Are Digital Twins Used in Industry?

Several large companies are taking advantage of either supplying the software to create DTs or designing DTs to improve product performance. A few companies profiled include Autodesk, ANSYS, PTC, Dassault, the Department of Energy, and the Department of Defense. Autodesk is leading the way with their new Autodesk MEP software that is designed to model DTs in architecture and building design. With Internet

of things (IoT) coming online, large systems and subsystems like HVAC and the power grid can give building owners and architects large amounts of data to integrate within architect software suites. Originally, buildings were modeled as DTs for strictly visual purposes, such as games or seminars, but today they have become interactive with a live data feed that can improve a building's performance by predicting maintenance cycles and degradation of the building itself. Figure 13 is a visual representation that Autodesk uses to showcase its architecture suite.



FIGURE 13: Representation of Autodesk Digital Architecture [16]

PTC is also well-versed in DT technology; its software suite is specifically designed for physics-based applications. Figure 14 is an image taken from their website.

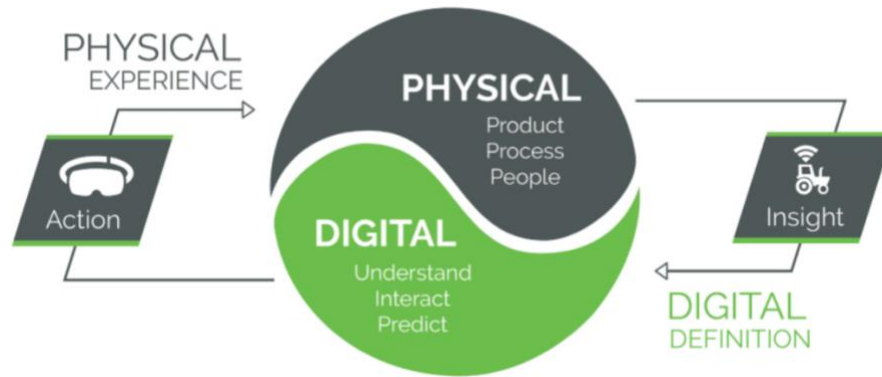


FIGURE 14: PTC Representation of DT [17]

PTC creates different software suites such as Creo and ThingWorx to implement DT technology that directly connects to smart manufacturing and IoT. Thingworx is the industry standard when it comes to DT platform architecture, PTC has created an entire suite to take advantage of IoT or smart manufacturing and can even turn the data into augmented reality to better display the results.

Dassault Systèmes is a French software company best known for its 3D CAD package SolidWorks. Dassault also owns the 3DSMAX software package, this software is used to model architecture and normal objects but without the physics getting involved. The company has recently thrown its hat into the DT arena. Below is an excerpt from their website explaining their new 3DexperianCity software:

Dassault Systèmes, for example, worked with the National Foundation of Singapore to create a complete virtual twin representation of the city using the 3DEXPERIENCity® solution. By combining geometric, topological, and environmental data with information on everything from climate to traffic

patterns, Singapore can run simulations and virtual tests to understand and develop solutions to urban planning challenges [18].

Figure 15 shows a screenshot of Dassault software on city planning by using different sensors to take real-time measurements, this type of data is how the smart grid can continuously improve upon itself.



FIGURE 15: Model of a City Using 3D Experience [18]

Figure 16 displays the simple concept of a motor transformed into a digital asset, this model can then be used to produce numerous simulations to provide data for smarter, more informed control. Motor systems are constantly evolving and need real-time feedback in order to improve the current draw, shaft torque, and bending loads. Similarly, digital models along with sensitive sensors can shed light on what works and what doesn't work inside an electric motor.

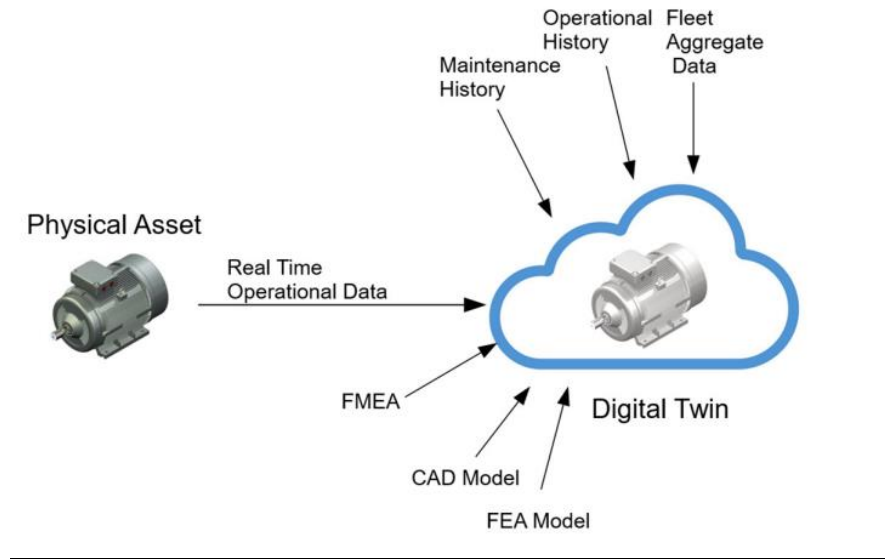


FIGURE 16: DT Representation [19]

DT technology is becoming more popular as time goes by. Having a digital copy of a real-life product can save a company millions of dollars compared to a traditional research and development process. Most car manufacturers take around six years to design and develop a new vehicle, which could be shortened by half just by implementing DT technology [19].

As DT technology advances software such as cloud business management systems (BMS) could aid in data storage and monitoring [20]. Cloud computing would strongly benefit an industry that seeks to harness the full potential of DT technology. Figure 17 displays an example of how the cloud service plus AI technology is integrated between real-life products and the digital reflection of that product.

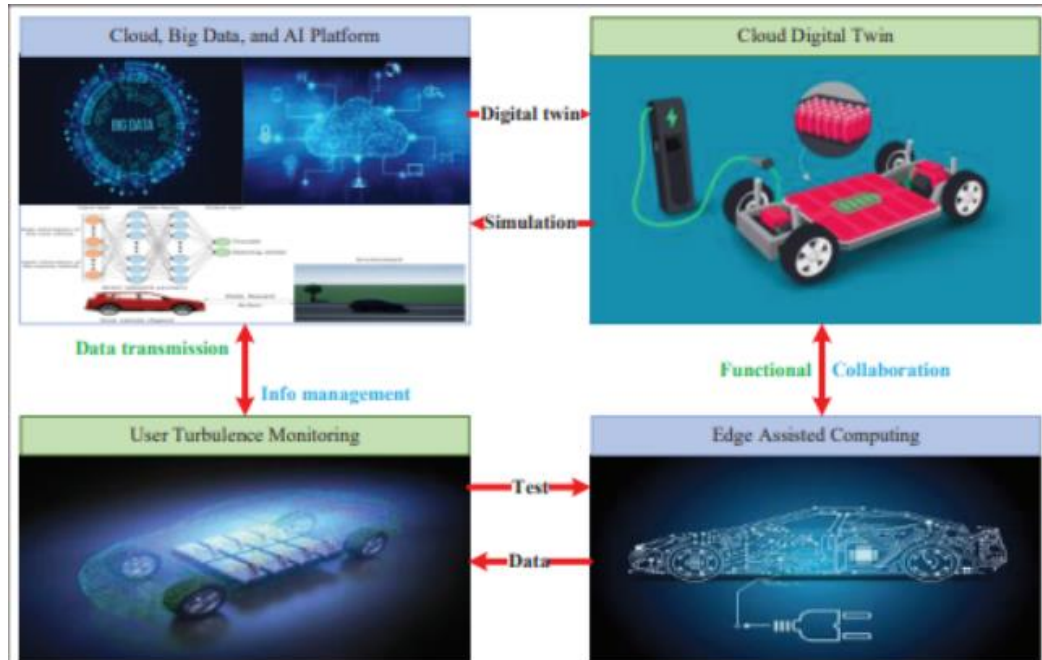


FIGURE 17: Cloud Integration of Big Data [20]

Figure 18 shown below explains in detail the levels or layers of cloud-based data acquisition that also includes other functionality beyond EV performance but also solar performance. The DT architecture shown below contains four layers. The physical layer corresponds to physical objects and conditions such as vehicle weight, solar panel surface area, road grade, and weather conditions. The connection layer includes sensors that collect data from the physical environment. The virtual layer is the virtual copy of the physical model; this includes the drivetrain and electrical components along with solar and external environmental elements. Finally, the service layer is the dynamic real-time monitoring of the DT that uses AI and specific algorithms to tweak and tune the data to fit a certain need [21].

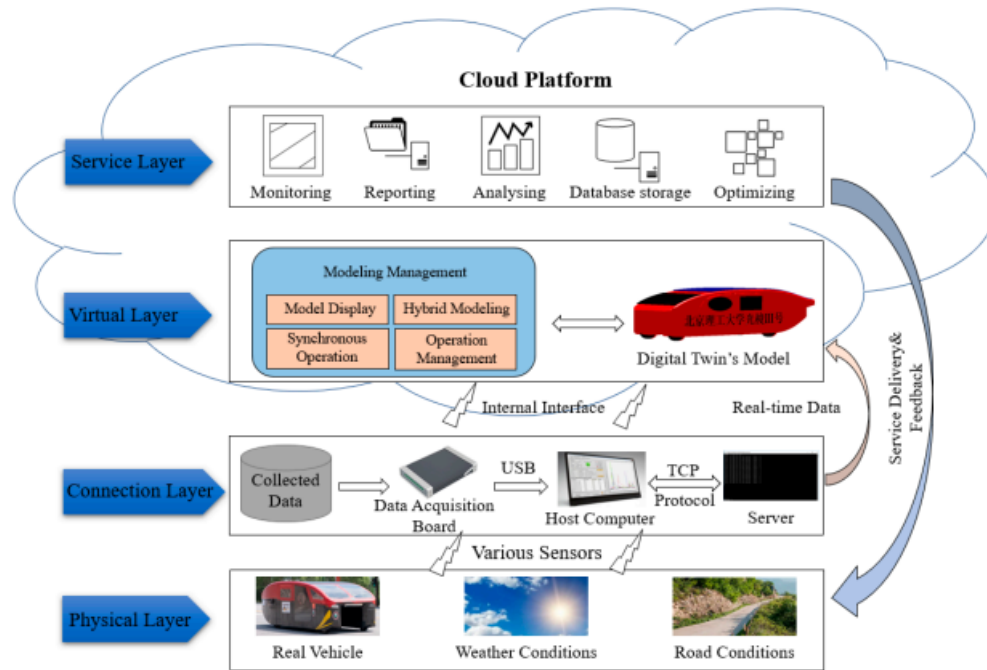


FIGURE 18: Service Layers [21]

In the vehicle design space, several software suites can provide deeper simulation data to help predict vehicle characteristics. VI-CarRealTime software is used to provide a robust package of dynamic vehicle data by supplying 14 Degrees of Freedom (DOF) physics vehicle models. This software, plus the addition of Simulink, provides a powerful tool in bridges several vehicle concepts together. Previous research used this software along with creating virtual simulations of track environments. Figure 19 shows a simulated track versus a real track [22].



FIGURE 19: Race Track Versus Simulation[22]

Figure 20 and Figure 21 represent how a digital model incorporating track data can be implemented. These figures display the vehicle's trajectory in three dimensions. In Figure 20 you can see both a top-down view and elevation data, which is used to create a more accurate depiction of a real track environment. Figure 21 displays the speed, power, and efficiency of the telemetry data of a real EV (red) versus a simulated DT of that vehicle (blue). There is general agreement between the models as the blue and red lines of the graph are very similar to one another, this shows the simulation was calibrated to fit the real-world model.

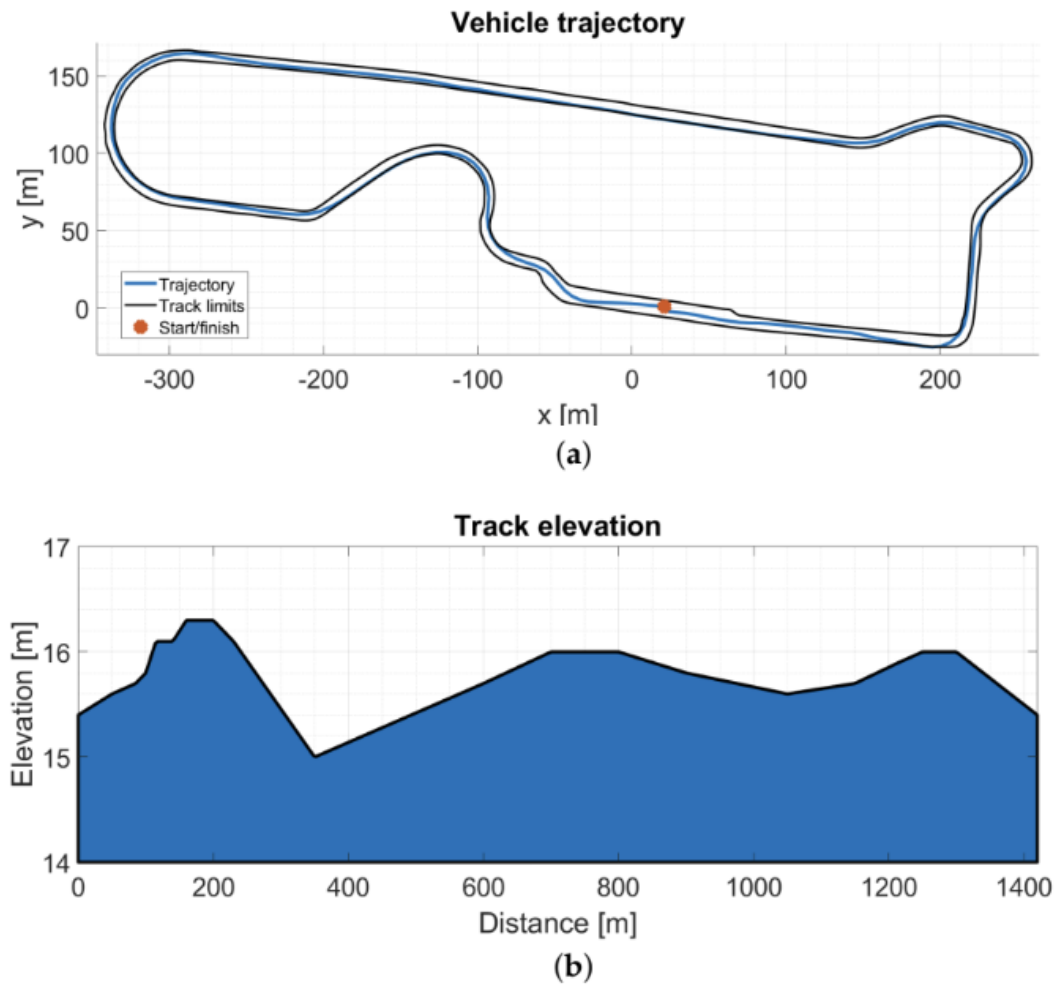


FIGURE 20: Vehicle Track Trajectory [22]

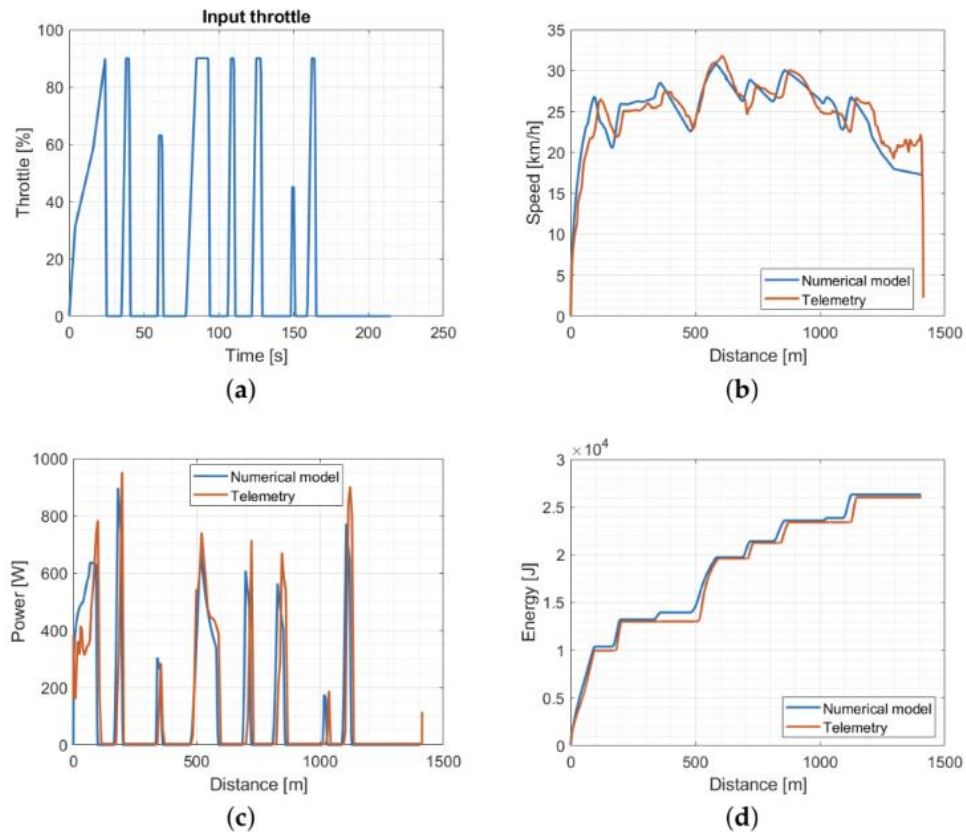


FIGURE 21: Telemetry Data Versus Real World [22]

Figure 21 shows the advantage of tracking physical models, this concept allows data to be viewed graphically to better understand the model's performance. Digital track data can precisely show faults in aerodynamics or engine performance. The faults can be corrected by viewing a simulation of the track environment. Track simulations can track a vehicle's physical trajectory along with the throttle response at given time intervals. Simulating different tracks along with varying vehicle modifications will deliver stronger data sets, these data sets can be used to predict future behavior.

CHAPTER 4: METHODOLOGY

The core of this research is to create a DT model of the Team Sunergy solar powered electric race vehicle. Simscape is the primary software used to create the EV model. Using this software, several systems will be modeled based on the previous data provided by the solar powered electric race vehicle. The model used in this research can have various outputs based on different inputs into the model. Figure 22 shows the model's inputs and output. The inputs include solar cell information, battery type, vehicle motor, type of vehicle body, the size of the vehicle wheels, the vehicle drag force, and course grade. The outputs the model will offer include vehicle distance, vehicle velocity, motor current draw, battery current draw, power consumption, power generation, and battery SOC. The main model will contain several subsystems that will exhibit the physics of certain components or operations in the vehicle.

Four specific subsystems are considered in this model of the solar EV ROSE. These subsystems were taken as the foundation of what a DT would need to simulate a true solar EV environment. The first model will include the solar array; this system will be the energy supplier for the EV. The second model will be the battery system; the battery system will transfer the energy generated from the solar system to the motor. The third system will include a model of the EV electric motor; the motor modeled in Simscape will include the same features as the motor on the EV. The fourth subsystem will include the vehicle dynamics; this model will include the tires, vehicle weight, drag, and elevation changes. The entire system will also be simulated on varying terrain grades in order to capture the data of a real racecourse.

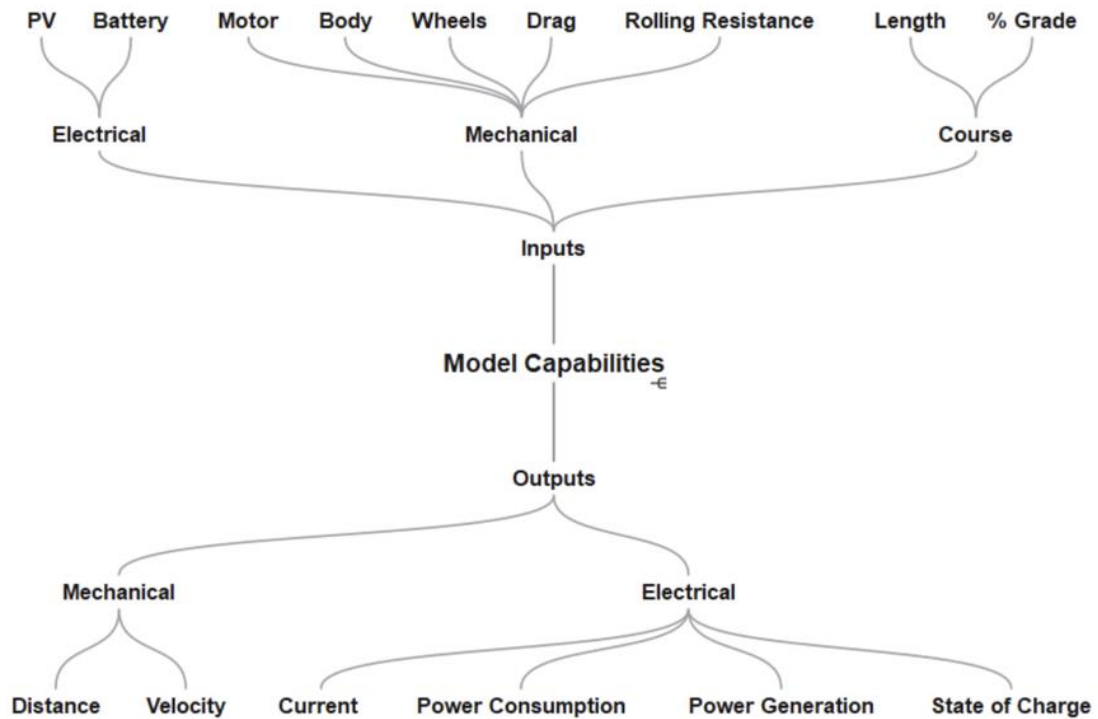


FIGURE 22: Model Capabilities

4.1 Physics-Based Modeling [System Architecture]

The solar powered racing EV DT takes several subsystems to output viable data that can be used in real-time simulation. Figure 23 and Figure 24 both represent a basic layout of how a solar powered EV would be pieced together. Using Simscape, a physics-based model was developed to accurately represent the real components of an EV vehicle. Ideally, a physics-based model would be represented by a single file or program. Unfortunately, an issue with the vehicle dynamics, PV solar array, and battery components caused compatibility errors and prevented the model from reliably solving as a single model. The current workaround was to have two separate models that are working together based on the data or current drawn from the motor. The motor data is

contained in the model shown in Figure 23. The current draw from the motor is sent to the solar cell and battery model shown in Figure 24 by a block called *out current draw*. Although there is no battery in the vehicle model, a stand in battery is used to simulate the charge being taken from the system. Figure 23 shows the stand in battery is set at *mVolts*; this value is a placeholder that can be changed through the settings initial function setup portal. As the motors run, Simscape will calculate the charge required to power the motor from the battery. The current draw from the motor is saved as data shown in blue; this block will export the current draw from the motor to the solar/battery model.

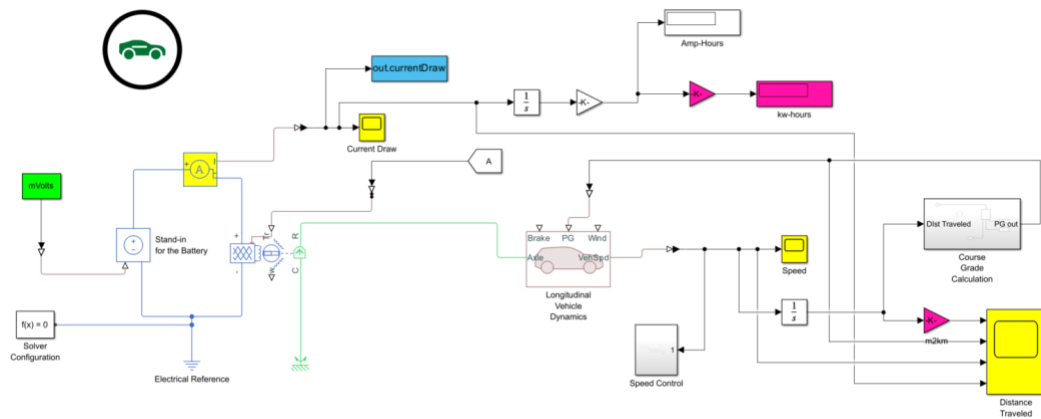


FIGURE 23: EV Dynamics / Motor Model

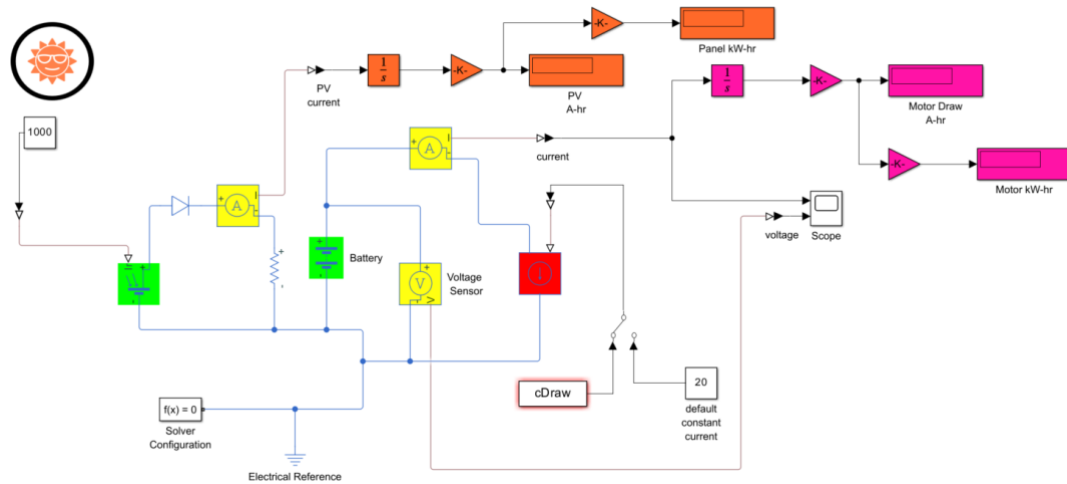


FIGURE 24: PV Solar Array /Battery Model

The out current draw function is the primary way the two models communicate. The vehicle model shown in Figure 23 is run first to populate the current draw from the motor, next the solar and battery model uses the vehicle data to run the solar and battery simulation. The model can incorporate varying levels of track grade. As the vehicle traverses different road gradients with varying incline degrees, the motor will require more current to stay at a certain speed. The amount of current that the motor will need based on achieving a steady speed is calculated by the PI control, the PI control parameters can be changed quickly to display different models that portray the EV behavior during a race. The entire model can display the battery's SOC based on input parameters, such as vehicle weight, vehicle set speed, drag coefficient, track gradient, solar panel capacity, type of motors used, and the number of battery cells used. Each block contained in the model can vary the simulation based on vehicle, battery, and solar characteristics. These characteristics can include vehicle weight, type of motor, type of battery, and type of solar cells used. Ideally what you want from a solar EV race car is

concentrated energy storage with as little vehicle weight as possible. The solar model described in the next section goes into the electrical architecture of the model.

4.2 Motor Modeling

The motor and drive block shown in Figure 25 is Simscape's electromechanical solution to integrate a motor that responds to electrical energy and mechanical energy. The motor block is modeled after a Mitsuba 2096M DC motor, and it has a rated output of 2000 W and weighs around 3.0 kg. The block has six total ports and of the six only five are used in this model. The first two ports located on the left side connect to the battery- in the current model's case, a stand-in battery, and the other two ports located on the right connect to the axle of the vehicle. The port located at the top of the block is the torque sensor. This port is useful in PI control since it can increase or decrease the motor performance based on the required torque at any given moment.

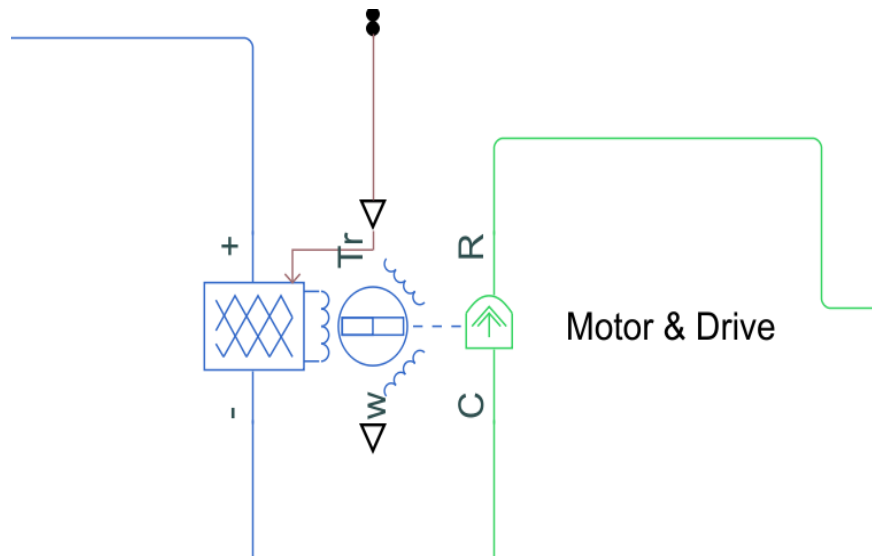
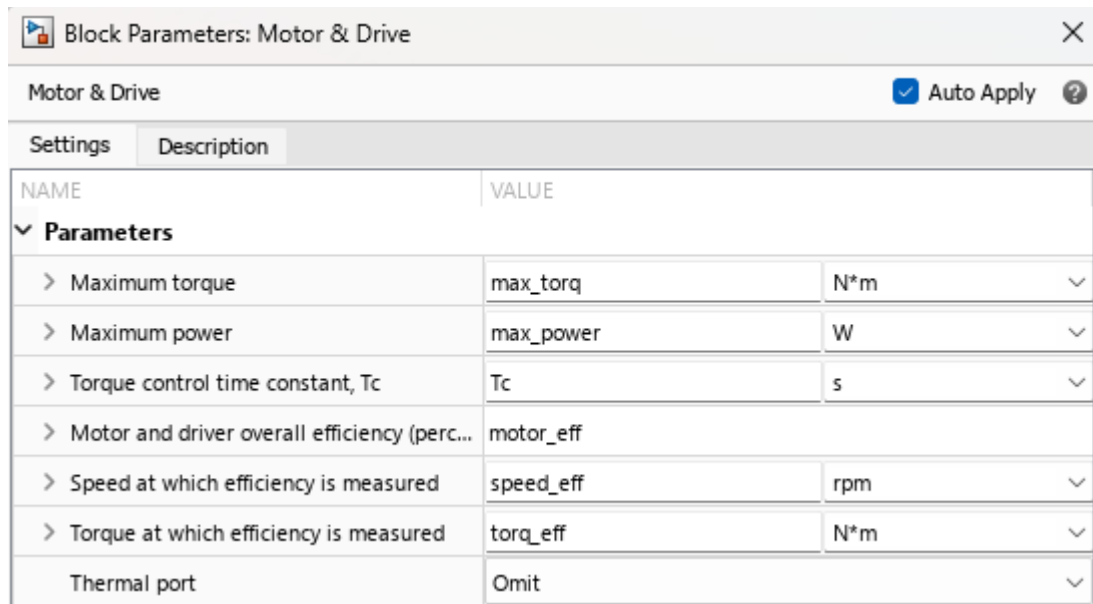


FIGURE 25: Motor Control and Drive

The parameters allow this model to be configured to match the motor parameters provided by Team Sunergy. The key parameters for this block include torque, power, and efficiency characteristics that are useful for basic modeling. Although Simscape does offer more advanced motor blocks, this model serves as a suitable initial representation of the real-life Team Sunergy's EV race vehicle.



NAME	VALUE	
Parameters		
> Maximum torque	max_torq	N*m
> Maximum power	max_power	W
> Torque control time constant, Tc	Tc	s
> Motor and driver overall efficiency (perc...	motor_eff	
> Speed at which efficiency is measured	speed_eff	rpm
> Torque at which efficiency is measured	torq_eff	N*m
Thermal port	Omit	

FIGURE 26:Motor Control Parameters

The mechanical rotation speed W is also an output on the block shown in Figure 26 but is not used in this model. The motor and drive system block is a hybrid physical model that can simulate the electrical and mechanical forms of energy; this type of modeling is convenient because the developer can easily transition from one domain to another without the need for lengthy calculations or complex interfaces. As electrical energy is entered into the motor port parameters, the energy is converted to mechanical torque; this torque is typically sent to a drive shaft or axle. Figure 26 displays how the control

parameters can easily be changed to modify the motor setup. See Appendix F for specific values used in the parameter box.

4.3 Vehicle Dynamics Modeling

The vehicle dynamics modeling block is the core of the model. The block is responsible for taking in several data points and combining them into one solid physics model. Figure 27 is the Simscape vehicle dynamics block. The vehicle dynamics block has several elements that make this block a powerful core of the vehicle physics model. The left-hand side of the block contains the axle node; this primarily receives data from another block such as a motor or a static set value and incorporates those values as a torque. The torque is then used in combination with tire parameters to produce vehicle speed.

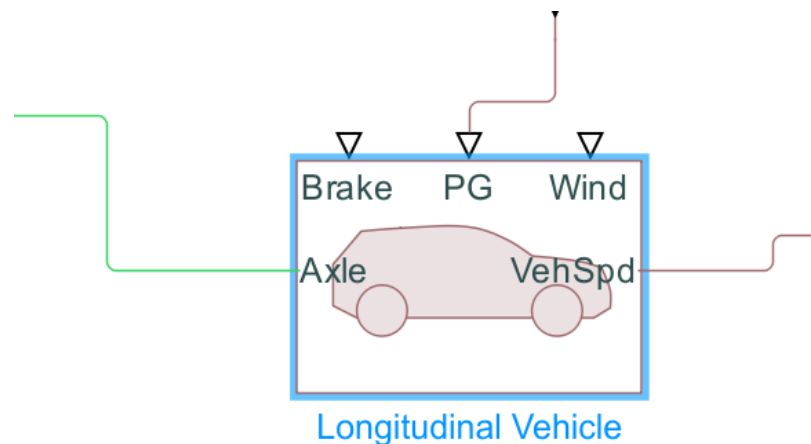


FIGURE 27: Longitudinal Vehicle Block

The percent grade (PG) node is a very powerful tool and a key feature of the DT. The PG function allows you to add a dynamic change in grade relative to a flat plane; this works

in the positive up-coordinate direction and the negative direction. This can be useful for race teams using a DT like this model, by taking the topography elevation coordinates from google maps or other positional applications, you can map out a racecourse's change in grade. This is a powerful advantage considering you can see in real-time what type of charge is leaving your system depending on the grade at that point.

Figure 28 is the parameter screen, which allows the modification of your vehicle by changing its mass, type of tires, drag coefficient, and frontal area of the vehicle that encounters most of the drag force. Simscape even offers default values for small, medium, and large vehicles- these options are good to test generic simulations quickly when vehicle parameters have not been specified. The two other nodes, brake, and wind will not be used in this simulation; they can be helpful in other applications but for this study, they have not been implemented. Figure 28 shows the parameter section of the vehicle block; this will determine vehicle dynamics.

NAME	VALUE
Vehicle	
Parameterization type	Regular parameter set
> Vehicle mass	v_mass kg
> Tire rolling radius	tire_radius m
> Tire rolling coefficient	tire_coef
> Air drag coefficient	drag_coef
> Vehicle frontal area	vehicle_area m ²
> Gravitational acceleration	9.81 m/s ²
Simulation	
Initial Targets	
Nominal Values	

FIGURE 28: Vehicle Block Parameters

Figure 29 displays how the speed is controlled on a high level. Figure 29 will also show the entire block diagram of the model to get a better view of how each block interacts with the other. Figure 30 is the PI control of the vehicle block. As the vehicle speed is sent out of the vehicle block the PI subsystem grabs that data at point A, and it then sends it to the error block where the current data is subtracted out by the set data point. The purpose of doing this is to control the speed of the vehicle since the simulation cannot have a real driver present. A set value is used to populate data. The set value, or speed, is 15 m/s but this value can be changed to any speed.

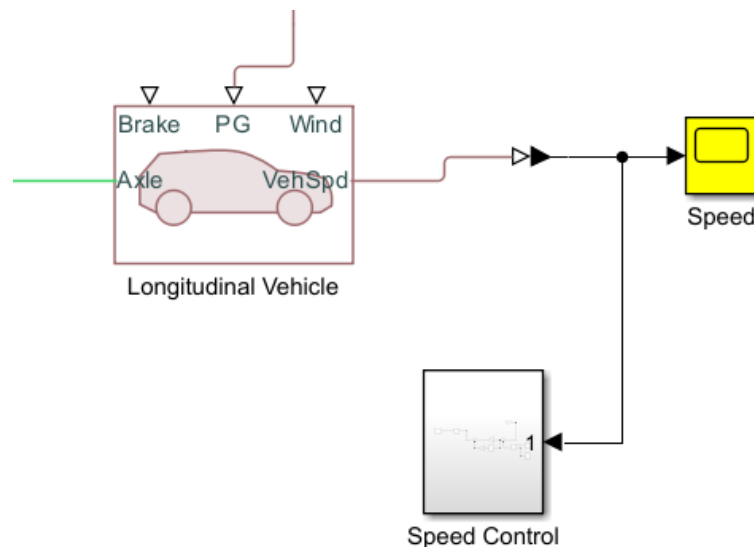


FIGURE 29: Vehicle Block with Speed Control

The data from PI control is sent to the A block, this block is used to transfer data from one model to another. This is shown in Figure 31. The data from the A block directly influences the torque going into the motor; this in return controls the speed. The feedback loop allows the motor to increase the current draw when the vehicle approaches a grade

level higher than zero degrees. When the vehicle is going downhill, the motor will use less energy since torque is not needed during that time. The PI control does not incorporate derivative functionality; only integrative and proportional control is used. Saturation was used to limit the model from generating a torque higher than what the DC motor can handle, this keeps the model in line with realistic results.

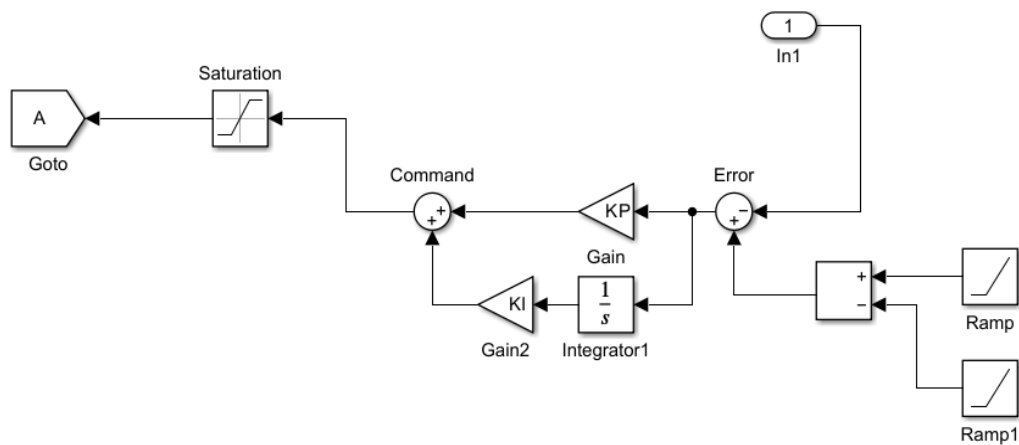


FIGURE 30: PI Control for Vehicle

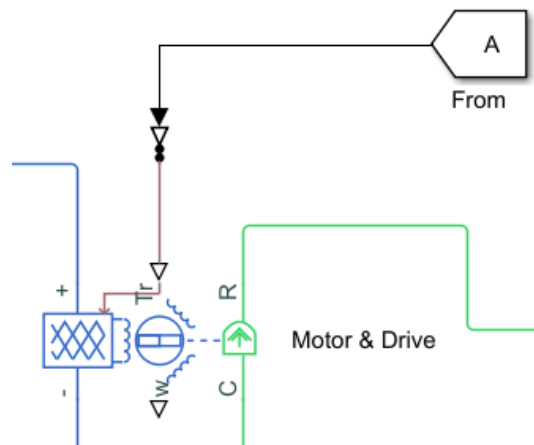


FIGURE 31: Data Entry from PI

4.4 Racecourse Modeling

The ability to model a racecourse and simulate the results is the focus of this research. This research will allow Team Sunergy to track the performance and energy usage across different terrain types. Racecourse modeling is combined into two categories; the first is flat track modeling and this type of modeling will give insights into the battery life and charge dissipation levels on flat surfaces. Since no grade is involved in the model, less current is needed by the motors to propel the vehicle forward. It is important to note that both the flat track and road course modeling are longitudinal models that do not include the impact of curves or stops in the simulation.

The second category is road course modeling, which introduces real terrain grade levels to give the model a more accurate depiction of how the vehicle will respond in real-life. This type of modeling is the most beneficial considering most tracks in competition contain large hills and valleys. Knowing the grade level can help predict the type of strategy ahead of time to win a race. The grade levels can be mapped into a data set by using mapping technology, such as google maps, or other third-party software available online. By knowing the grade and distance, a simple matrix can be set up to import the data into a format MATLAB can recognize, this data can be used to simulate a track environment.

4.5 Flat Track Modeling

Flat track modeling is used to test certain parameters without using elevation changes; it primarily runs the model without using complicated calculations. This is handy for prompt calculations. Flat track modeling does not implement grade when calculating motor current draw. Figure 32 exhibits the road course modeling system when

grade is not used, the model calculates the amount of charge stored in the battery throughout the trip.

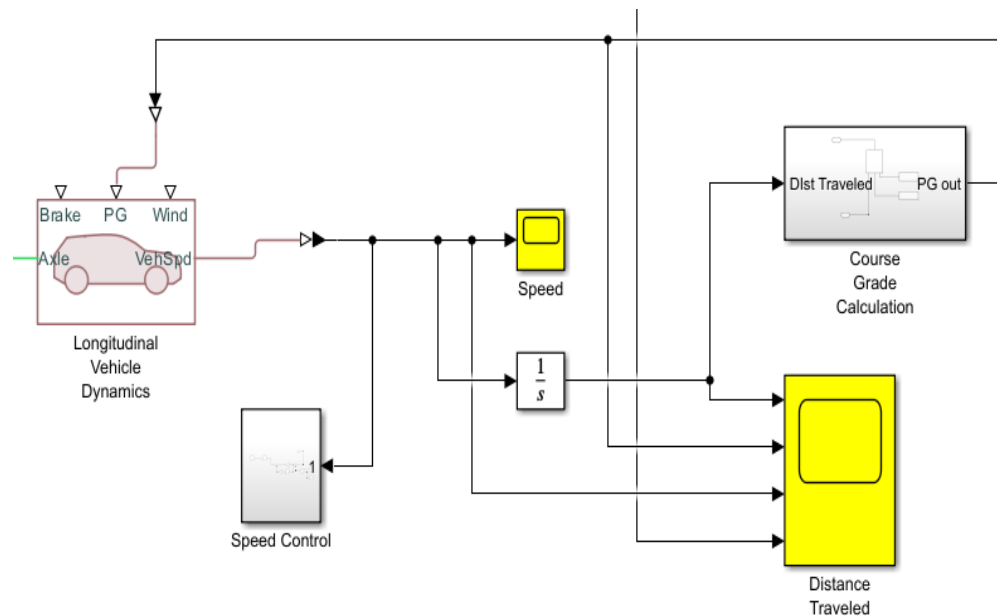


FIGURE 32: Road Course Model System

4.6 Road Course Modeling

The road course modeling uses several data sets to calculate the PG. To have an accurate model of terrain, a certain number of data points will be needed; these data points include the distance from a starting location and the elevation level on each unit of distance traveled. This data can be obtained from third-party applications that map specific roads, highways, or tracks. As the accuracy of the input data increases, so does the model. The model uses CSV files to easily upload and store the data used for track or road course mapping. Figure 32 demonstrates the specific functions in the simulation used to calculate the grade percentages used in determining the track performance of the EV.

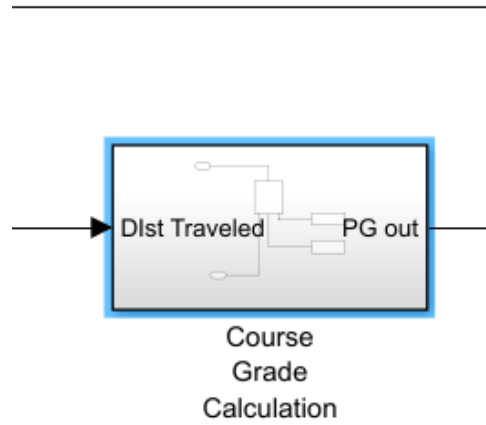


FIGURE 33: Course Grade Calculation

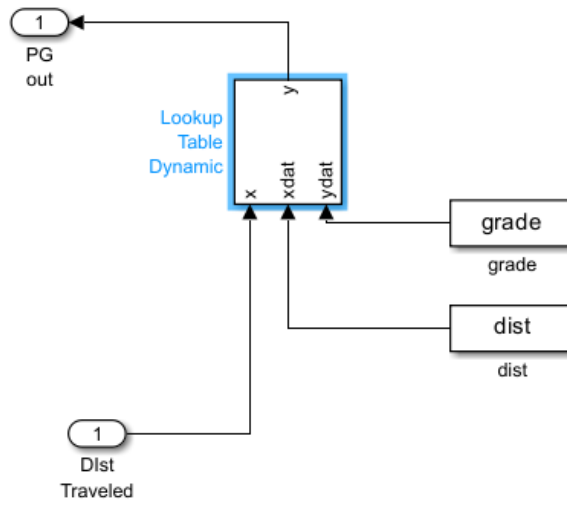


FIGURE 34: Course Grade Sub System

```
dist=[0 1000 2000 3000 4000 7000 9000];  
grade=[0 0 2.5 4 3.5 0 -1];
```

FIGURE 35: Sample Distance and Grade Value Matrix

Figure 33 is a subsystem of the course grade calculation. This block pulls in data from the vehicle block such as distance traveled and inserts it into a look-up table shown in Figure 34. The distance traveled and grade values are inserted into matrix format as shown in Figure 35. The lookup table has three inputs and one output. The x value is the relative position of the vehicle, the xdat entry is the distance variable, and the ydat is the grade variable. Both the xdat and ydat are managed as a matrix function through MATLAB. The matrix data set is a function called when the lookup table is used. Once the three inputs are entered into the data table the output is sent to the vehicle block as a PG data point. Once the vehicle block receives the PG data point it calculates a new velocity for the vehicle. Higher grades will also reflect in the current draw as well as the velocity.

4.7 Solar Panel Modeling

The solar array and battery model are dependent upon the execution of the vehicle model. Since the solar model is dependent upon how much energy leaves the battery, the vehicle model is run first to calculate the energy needs for the EV. The amount of energy taken out of the system is then sent to the solar and battery model where the solar and battery function blocks calculate the appropriate graph to show the SOC of the battery.

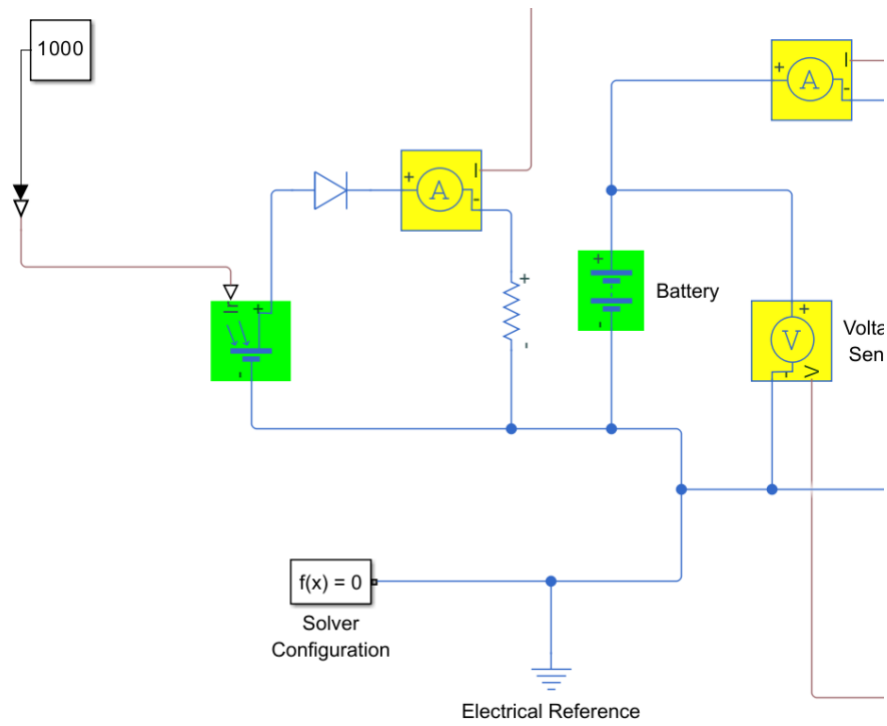


FIGURE 36: Solar PV System

Figure 36 displays how the solar to battery electrical system works. The PV array shown in Figure 37 is a Simscape block that takes the traditional solar array network and condenses it into a single block. This cuts down on the number of blocks used in the Simscape architecture.

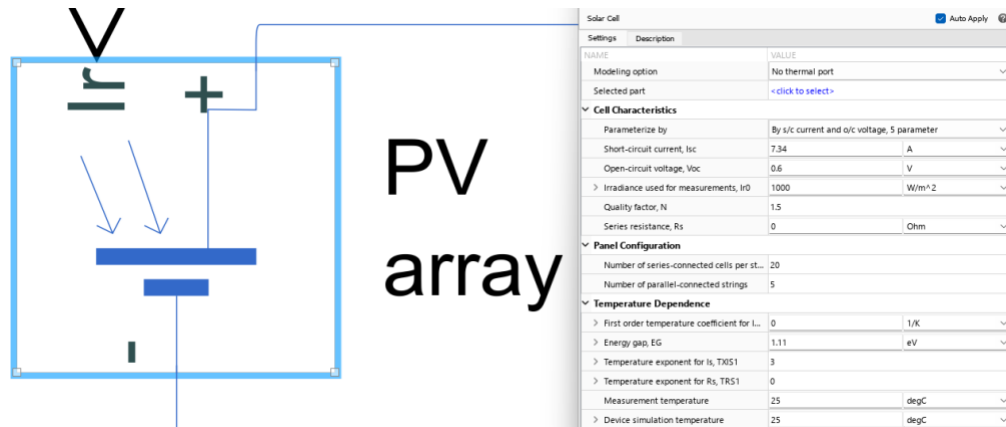


FIGURE 37: PV Solar Array

The solar block has three main connections, an input of irradiance, and two electrical connections. The irradiance can be entered as a set value, or a more dynamic approach can be taken to vary the sun's irradiance depending on the time of day and the position of the sun in the sky.

The screenshot shows the 'Block Parameters: PV array' dialog box. It has a title bar with a close button and an 'Auto Apply' checkbox which is checked. Below the title bar are two tabs: 'Settings' (selected) and 'Description'. The main area is a table with columns 'NAME' and 'VALUE'. The parameters are grouped into sections: 'Cell Characteristics', 'Panel Configuration', and 'Temperature Dependence'. Each parameter has a value field and a unit dropdown menu.

NAME	VALUE	UNIT
Modeling option	No thermal port	
Selected part	<click to select>	
Cell Characteristics		
Parameterize by	By s/c current and o/c voltage, 5 parameter	
Short-circuit current, Isc	7.34	A
Open-circuit voltage, Voc	0.6	V
Irradiance used for measurements, Ir0	1000	W/m ²
Quality factor, N	1.5	
Series resistance, Rs	0	Ohm
Panel Configuration		
Number of series-connected cells per st...	20	
Number of parallel-connected strings	5	
Temperature Dependence		
First order temperature coefficient for I...	0	1/K
Energy gap, EG	1.11	eV
Temperature exponent for Is, TXIS1	3	
Temperature exponent for Rs, TRS1	0	
Measurement temperature	25	degC
Device simulation temperature	25	degC

FIGURE 38: Solar PV Parameters

The Simscape solar cell parameter block is convenient in the fact that you can customize a solar cell all in one block. This can lead to rapid solar cell testing without the need to add dozens of cells in parallel or in series to achieve a certain power output. The parameter menu allows the user to set the number of cells that need to be used in the calculation. Looking at Figure 38 and Figure 39, Simscape offers a repository of solar PV cells that have manufacture data already prepopulated; this option is in the selected part section.

Part number	Manufacturer	Physics	PanelType	Pm,W	Voc(STC),V
AS_6M30_HC_32	Amerisolar	Mono-crystalline Si	Half cell	320.0000	40.2000
AS_6M_360W_PE...	Amerisolar	Mono-crystalline Si	Full cell	355.0000	47.4000
AS_6P30_HC_280W	Amerisolar	Poly-crystalline Si	Half cell	280.0000	38.6000
AS_6P_HC_340W	Amerisolar	Poly-crystalline Si	Half cell	340.0000	46.2000
AS_6P_HC_360W	Amerisolar	Poly-crystalline Si	Half cell	360.0000	47.0000
ThinFilm_AS_100W	Amerisolar	Amorphous Si	Full cell	100.0000	115.8000
ThinFilm_AS_85W	Amerisolar	Amorphous Si	Full cell	85.0000	114.2000
CHSM5001T_110W	Astronergy	Amorphous Si	Full cell	110.0000	134.9000
3C44_30sqmm	AzurSpace	GainP/GainAs/Ge	Ge substrate, at 250 concentration	12.0000	3.0800
3C44_9sqmm	AzurSpace	GainP/GainAs/Ge	Ge substrate, at 250 concentration	3.9200	3.0500
CV1_80_3	Calsonic	CuTe	Thin film	80.0000	88.0000

Attribute	Value
Manufacturer	Amerisolar
Part number	AS_6M30_HC_320W
Part series	
Web link	http://www.weamerisolar.com/
Part type	320.00W, Mono-crystalline Si, Half cell, Voc=40.20V, Isc=10.14A, Vm=33.40
Parameterization date	06-Dec-2021
Parameterization note	Predefined parameterizations of Simscape components use available data s
Part data file location	Sources\Solar_Cell\Amerisolar\AS_6M30_HC_320W.xml

Parameter name	Parameterization	Override	Part value:AS_6M30_HC_320W	Present block value	Unit
Cell Characteristics>Short-circuit current, Isc	Datasheet derived	<input checked="" type="checkbox"/>	10.14	7.34	A
Cell Characteristics>Open-circuit voltage, Voc	Datasheet derived	<input checked="" type="checkbox"/>	0.67	0.6	V
Cell Characteristics>Diode saturation current, Is	Datasheet derived	<input type="checkbox"/>	0	0	A
Cell Characteristics>Diode saturation current, Is2	Datasheet derived	<input type="checkbox"/>	0	0	A
Cell Characteristics>Solar-generated current for mea...	Datasheet derived	<input checked="" type="checkbox"/>	10.14	7.34	A
Cell Characteristics>Irradiance used for measureme...	Datasheet derived	<input type="checkbox"/>	1000	1000	W/m^2
Cell Characteristics>Quality factor, N	Datasheet derived	<input checked="" type="checkbox"/>	1.51118	1.5	1
Cell Characteristics>Quality factor, N2	Datasheet derived	<input checked="" type="checkbox"/>	2.60259	2	1
Cell Characteristics>Series resistance, Rs	Datasheet derived	<input checked="" type="checkbox"/>	1e-05	0	Ohm
Cell Characteristics>Parallel resistance, Rp	Datasheet derived	<input checked="" type="checkbox"/>	682.95993	Inf	Ohm
Panel Configuration>Number of series-connected cel...	Datasheet derived	<input checked="" type="checkbox"/>	60	20	1

FIGURE 39: Solar Cell Manufacturer Datasheet

The remaining solar cell parameters can be modeled given the correct data such as cell characteristics, panel configuration, and temperature dependence. The solar PV block irradiance for this model is set to 1000 W/m^2 . This value was selected as a base value; but can be adjusted to represent the actual energy levels captured. Actual solar array data was modeled from MAXEON GEN III cells; this data sheet can be found in Appendix I. The total power output from the solar cells totals 1.2 kW with 326 total cells covering ROSE. Appendix J has more details on the solar cell energy output.

4.8 Battery Modeling

The battery model is a relatively new block that was added to Simscape in the 2022 release; it offers some basic parameters as well as custom functionality for different applications. The battery block natively contains a node for displaying SOC and can be easily connected to basic electrical sensor blocks to measure voltage and current.

Although battery systems can range in complexity and design, and sometime serve as the

focus of complex Simscape models, the default Simscape battery block has the key features needed for modeling an EV race car.

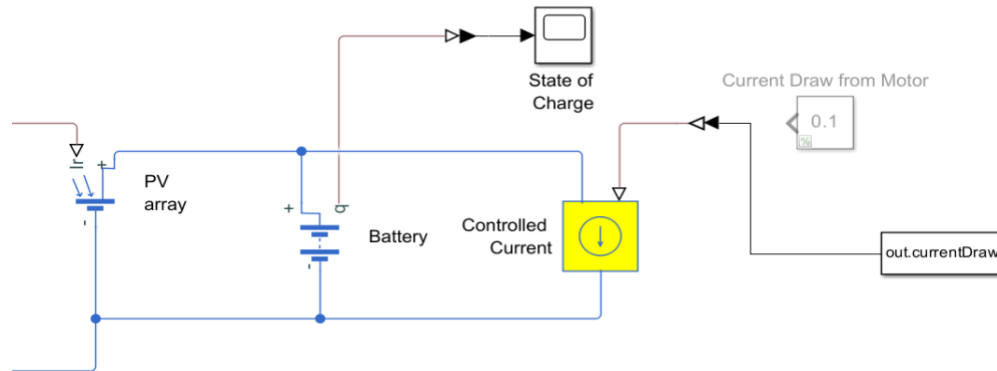


FIGURE 40: Battery Block System

Figure 40 is the top-level view of the battery block system and its connections. The battery system receives charge from the solar array block, and it also contains a controlled current block that pulls current from the battery from the vehicle model. The vehicle model will simulate different grades on a racecourse; during different grade changes the vehicle will require more energy to be pulled from the battery. Once the data from the vehicle model is complete, it is sent to the battery model where the controlled current pulls charge from the battery by implementing the *out.currentDraw* function. The *out.currentDraw* function is the link between the vehicle model and the battery model. As the data changes in the vehicle model, the *out.currentDraw* will import that data into the battery block.

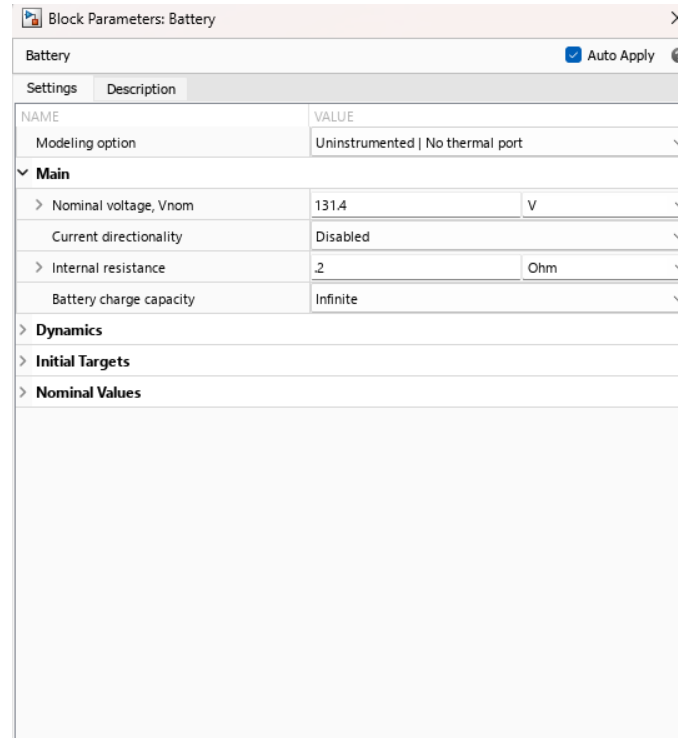


FIGURE 41: Battery Block Parameters

The parameters for the battery are simple in scope and relevant to the functionality of this model. Figure 41 shows the battery parameters and some of the custom options that can be set for different scenarios. Although the battery parameter block allows for a wide variety of customizability, the charge capacity setting is set to infinite for this model due to the lack of detailed battery information. The state of charge of the battery is determined by coulomb counting or current integration, where the current draw from the battery is integrated over time. This integrated value represents the number of amp-hours (or kW-hours) that have been depleted from the battery and can be compared to both the battery capacity and rate of recharge from the solar panels.

CHAPTER 5: RESULTS

The research performed on this project shows how DT models can be a powerful tool for design and engineering, especially performance-based applications. The research findings are, first and foremost, to show the capability of DT software, such as Simscape, and how it can be further refined to present an accurate depiction of a physical model. Although the model shows a rich representation of how a battery's charge can be affected by road grade and solar charging capacity, it does not offer a perfect or complete model of the EV. Continued research would be needed to refine the parameters to increase the fidelity of the model.

5.1 Track Simulation

The results of the model can be viewed for three types of courses; a flat road course model where no elevation change is present, a racecourse model where a constant grade is present, or a race course where the grade changes as a function of distance along the course. Figures 23 and 24 show a complete model of the DT system. Figure 23 is the vehicle model and Figure 24 is the solar/battery model. Originally, both the vehicle and solar/battery model were in the same file, but due to solver complications, the model had to be separated for it to run correctly. To run the simulation, the vehicle model needs to populate the data required to accelerate the vehicle forward, and this data is taken from the motors that power the EV.

The data from *out.currentDraw* is exported to the second model, the solar/battery model. Figure 42 shows the data that is imported from the vehicle model as *cDraw*. Once the data is imported into the model, Simscape subtracts the current draw from the battery,

and as the battery is drained of current from the vehicle model the solar pack adds power back into the battery.

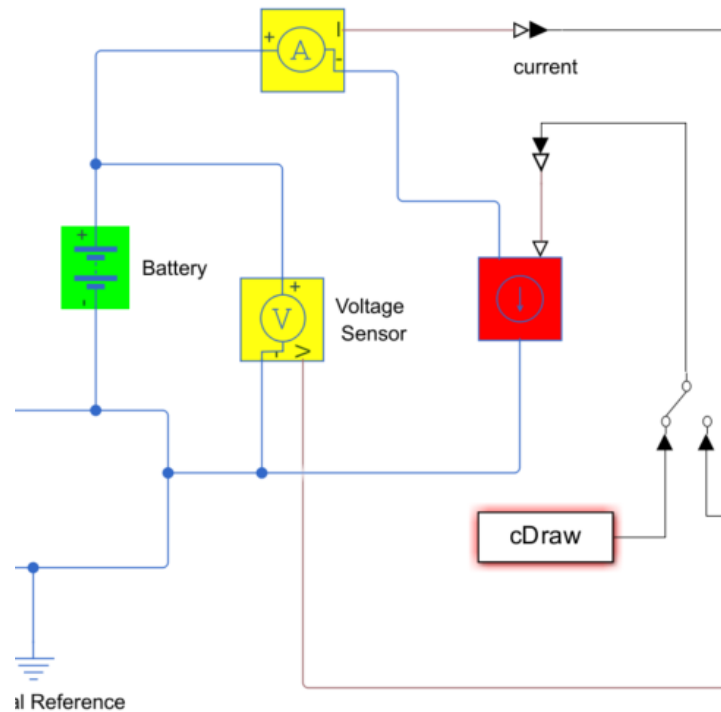


FIGURE 42: Solar/Battery Model

Figure 43 is a snapshot of the current draw with no grade, this data is taken from the vehicle model's current draw block. The run time for this simulation is 500 seconds and the peak current draw is around 37 A. According to the motor data sheet found in Appendix A, each motor has a max current draw of 25 A and two motors have a total current draw of 50 A.

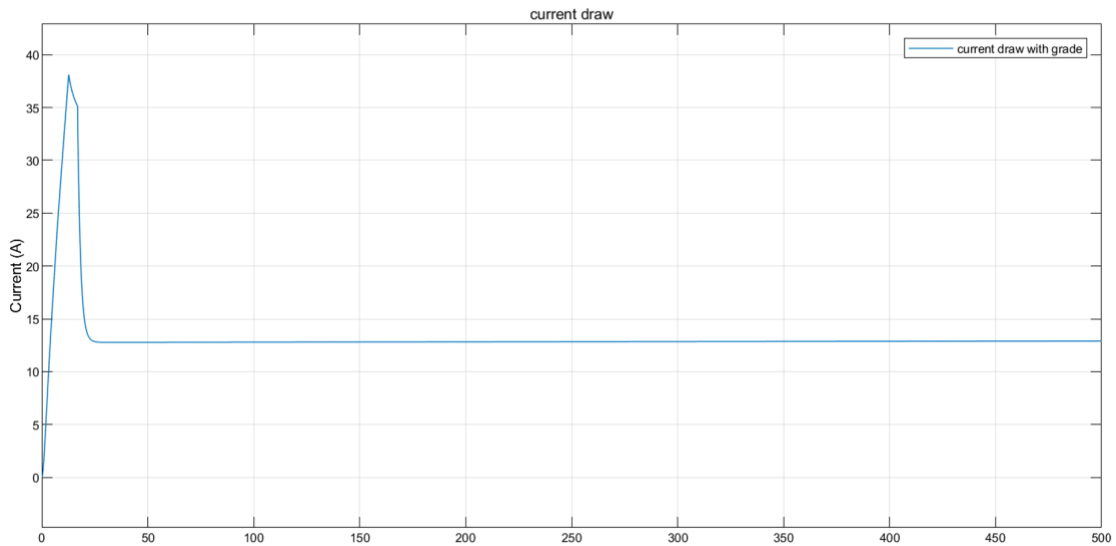


FIGURE 43: Current Draw No Grade As Measured in the Vehicle Model

Figure 44 exhibits the results of running the solar/battery simulation with no grade. The current data was imported into the model from the vehicle model. The top graph displays the current pulled from the motor and the bottom displays the battery's voltage drop. The initial current spike peaks around 37 A and settles around 16 A. With no incline present, the model displays a smooth flat line indicating the remaining run time had zero to no current pulse. This is expected on a flat plane with no varying changes in wind resistance. The voltage shows a similar representation as the current above. The voltage flat lines around the 25 second mark and stays flat during the duration.

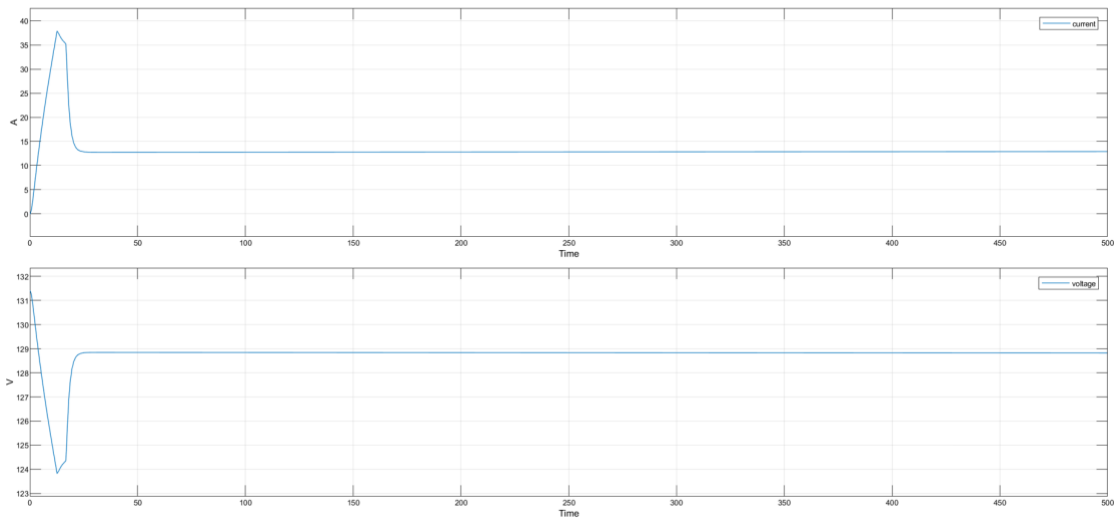


FIGURE 44: Current and Voltage No Grade in the Battery/Solar Panel Model

The irradiance of this simulation was set to a default value of 1000 W/m^2 ; this value in real-life is constantly changing depending on the sun's angle and cloud coverage. Figure 45 displays several data points that the simulation captures from the EV model. The model's runtime is 500 seconds to better display the graphical pulses. The first graphical display is distance; distance will depend on the time set for the simulation. The second data section is PG, but since this simulation is a flat track no grade was present. The third section is the vehicle velocity, and this section helps identify the rate of movement on certain areas of the track. The final section is the current draw; this factor will change dynamically when different grade levels are present.

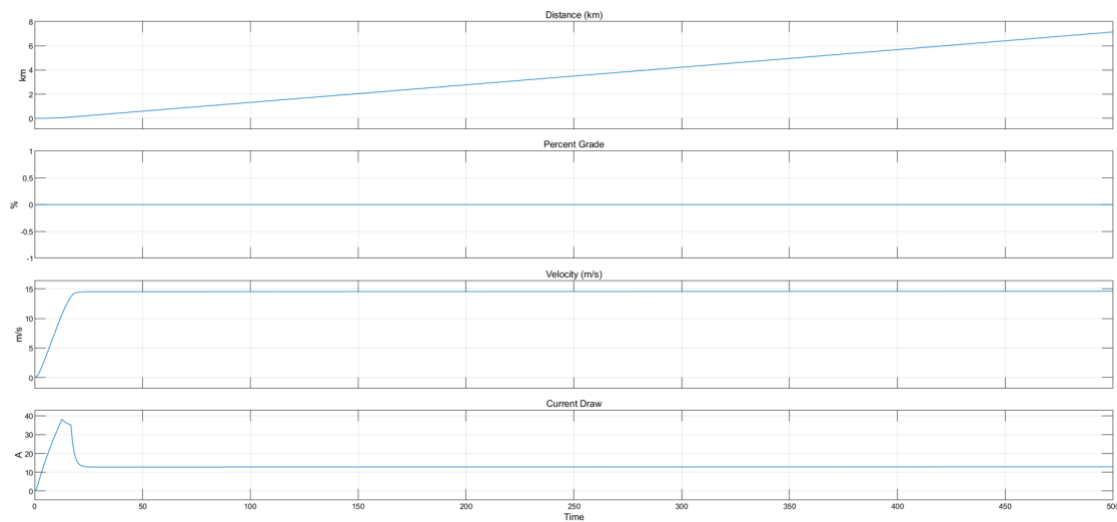


FIGURE 45: Multi Data Chart with No Grade.

5.2 Course Simulation

The data shown in the flat track simulation displays a simple model to current in and out of a system. Most road surfaces are not flat and have varying degrees of grade present, therefore, to display how the simulation works on unlevel road conditions a bike track geo-locational software was used to calculate the distance and elevation changes from the University of North Carolina Charlotte to Appalachian State University. The website can be found in Appendix G and Appendix H for further information. Using the elevation and distance data, over 235 data points were collected and transformed into a CSV file that can easily be read by Simscape. The raw data is then transferred into matrix format using the functions in Figure 46.

```

T= readtable('fullCourse.csv');
G= T{:,2}
dist= G(:,1)'
grade=G(:,2)'

```

FIGURE 46: MATLAB Data Matrix Functions

The data within the matrix is taken and transferred into two data sets, *GRADE*, and *DIST*; these variables are used to calculate the PG shown in Figure 47. The dynamic lookup table in Figure 48 takes the *GRADE* and *DIST* data and subtracts it from *X*, which is positional data from the model; the result is *Y* data that is inserted into the vehicle longitudinal block. The *Y* variable is filtered to remove outliers.

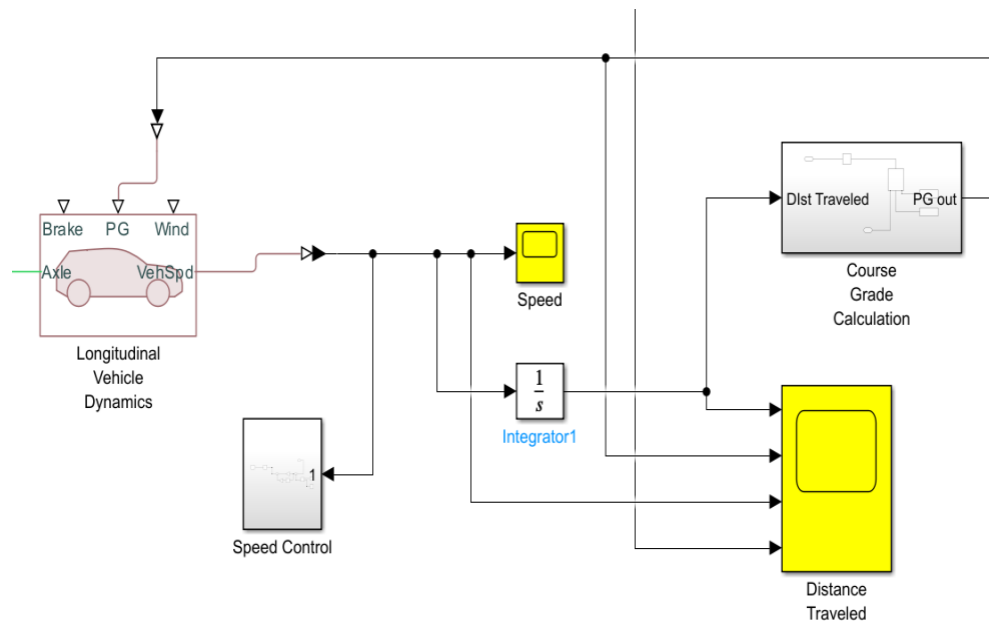


FIGURE 47: Vehicle Model

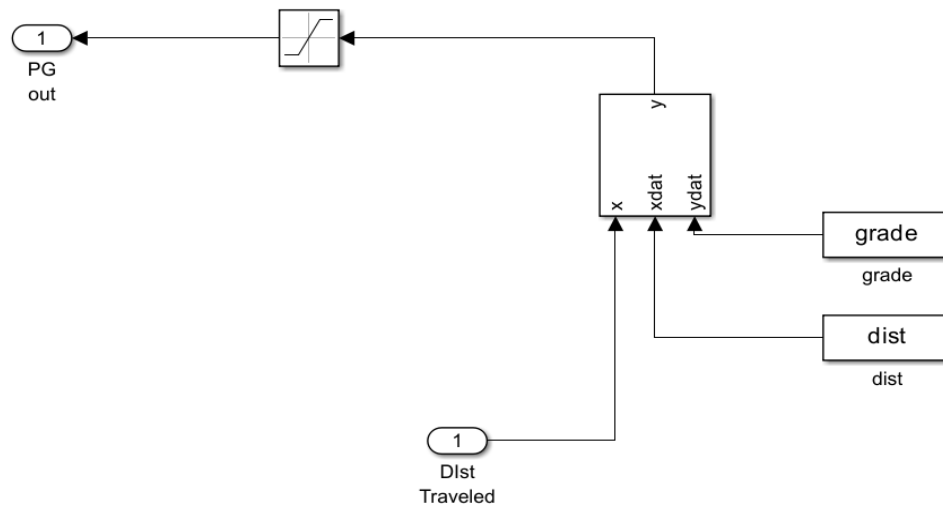


FIGURE 48: Grade Model

As the vehicle accelerates, any grade change will immediately pull more current from the motor. There are three simulations that utilize the model architecture, each simulation is set up differently to display differing results. The first simulation involves random grade changes; this is to show how the model displays data based on drastic elevation changes. The second simulation utilizes actual data taken from a third party, this data contains the distance and elevation change from UNCC to Appalachian State. The third simulation is the same as the second but in reverse. Since Appalachian State is located at a higher elevation than UNCC, a model in reverse would show the results of a negative slope environment.

Figure 49 represents the first simulation with a non-zero grade. The graph is broken into four sections; the first shows the distance traveled measured in m/s , the second section displays the PG in a graphical format, and the PG is the distance versus

the elevation change. This simulation uses an arbitrary course profile with sharp elevation changes to display how the other model components react, such as the vehicle and battery model. The graph shows that as the grade level increases there is a corresponding rise in the current drawn by the motors. As the vehicle climbs a hill naturally more current is spent to overcome the gravitational force of the vehicle's weight. This simulation is set to a run time of 7200 seconds and a total distance of over 100 km. The graph gives insight into where the motor pulls the most current and verifies basic operation. Having accurate road course data will allow the model to display the larger current spikes; these larger spikes can be better managed by adjusting the PI control and this will allow for better battery performance during a racing environment.

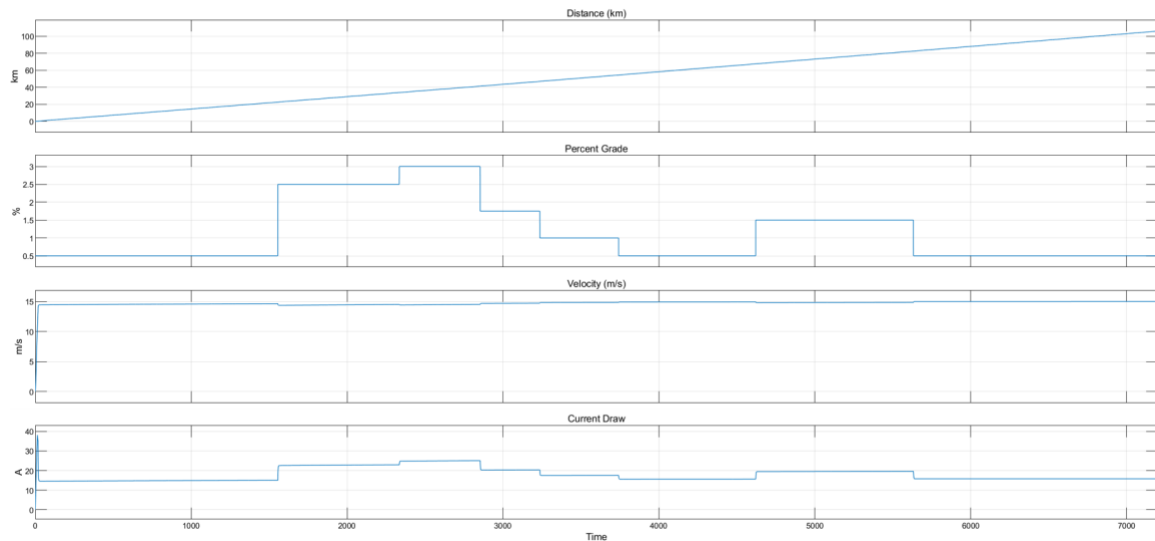


FIGURE 49: Vehicle Characteristics for an Arbitrarily Changing Slope

Following the successful simulation of an arbitrarily changing slope, a series of constant slope simulations were performed. Figure 50 plots the amp-hours expended over the course of a two hour simulated run, as a function of increasing grade change. The levels

of grade change range from -3 to 3 degrees; each grade degree or slope is attached to its corresponding amp hour current draw from running the simulation.

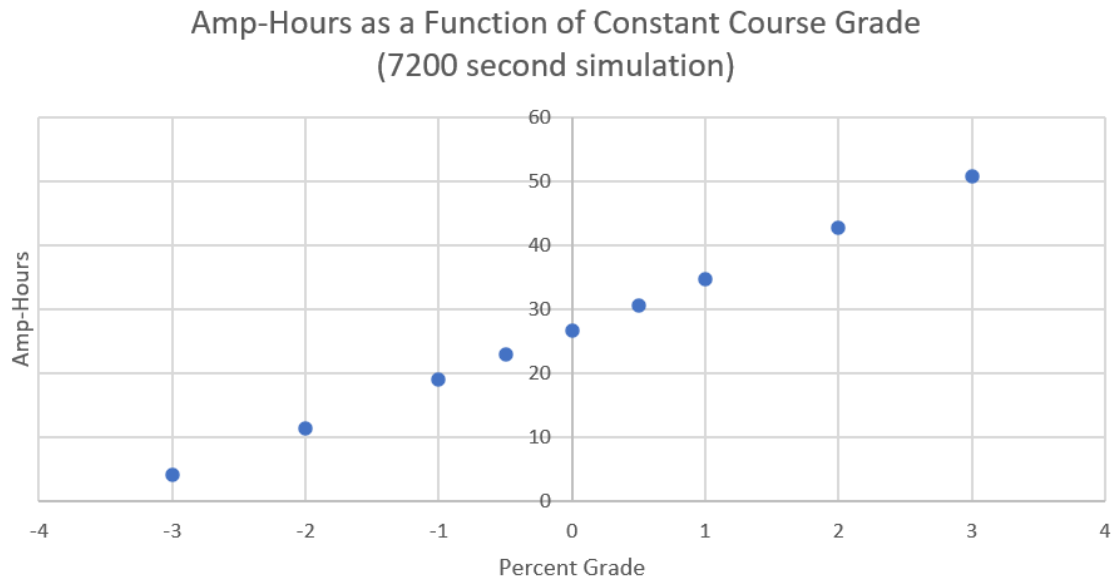


FIGURE 50 Amp Hours as a Function of Grade

Figure 51 is a representative graph from the constant slope simulation; the purpose is to show current and velocity output results for slopes set at a certain angle that do not vary. This simulation is useful for determining how the vehicle and motor system handle long stretches of continuous incline. In reality, most inclines neither last two hours or stay at a consistent grade but the data can be useful when the model settings are set to a shorter period of time.

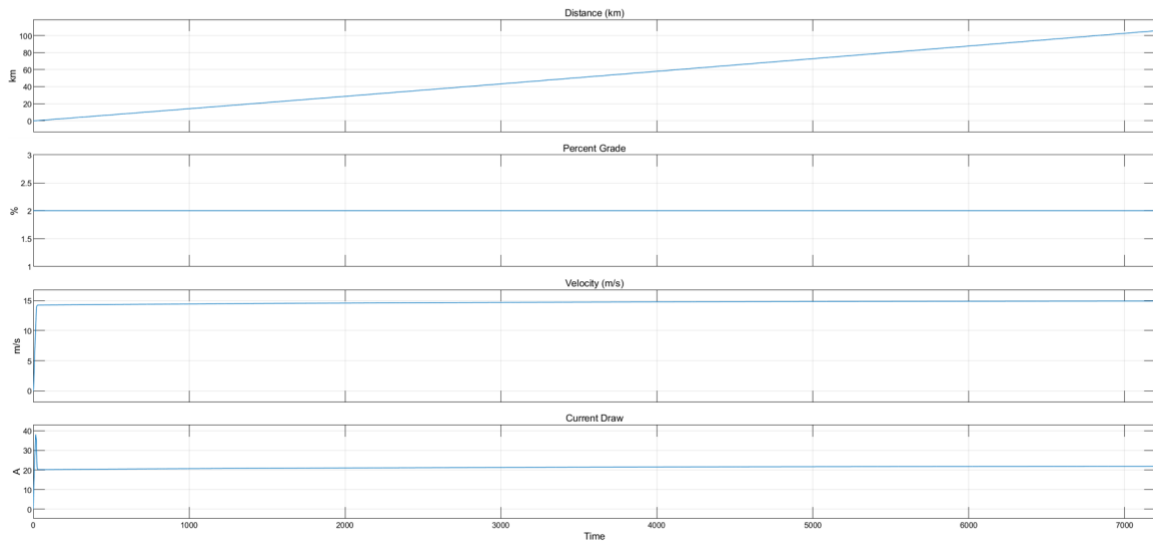


FIGURE 51 Constant Slope Simulation Dashboard

Having accumulated successes with flat tracks, arbitrary slopes, and constant slope simulations, the final simulations would use actual elevation data to determine the percent grade as a function of distance along the course. Figure 52 tracks actual track/road data from UNCC to Appalachian State. The purpose of this model is to track how much energy usage is required to traverse a certain landscape; this helps predict future tweaks in motor performance and what kind of load can be expected from the battery and solar cells. The chart shows the road or track from UNCC Charlotte to Boone North Carolina has several hills and valleys. The third section shows the change in velocity; as higher grades are encountered the vehicle will naturally lose velocity. The last section is the current draw, which shows exactly where on the track the most current was pulled from the battery. This information gives insight into how to manage energy reserves effectively.

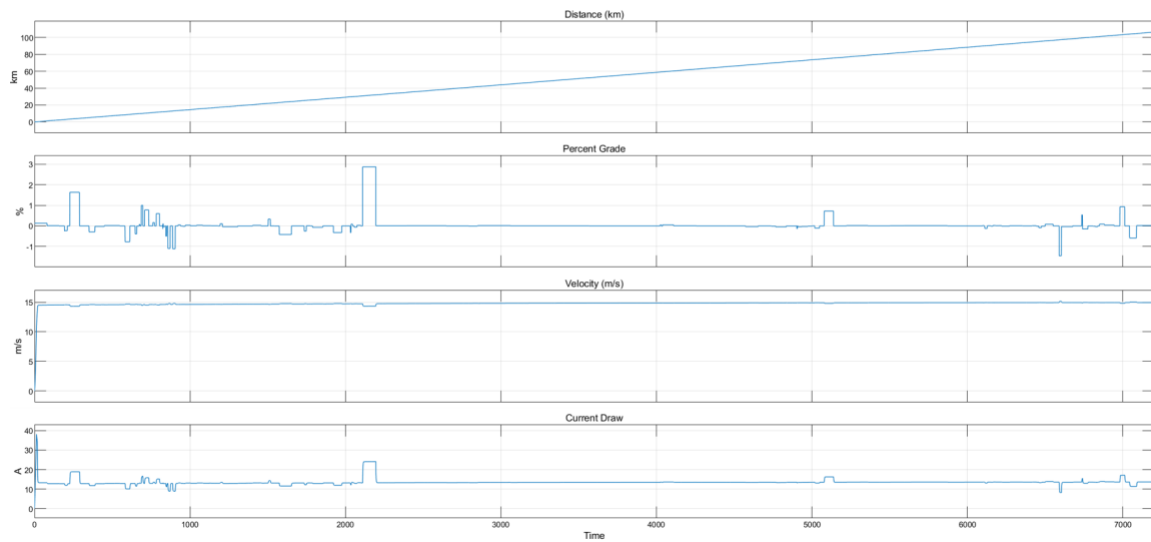


FIGURE 52: Vehicle Characteristics of Simulation Two

The data from the vehicle model is transferred at the same time to the battery/solar model. Figure 45 shows the data coming into *cDraw* from *out.currentDraw*. Figure 53 shows the voltage and current being taken out of the battery. Looking at the voltage and current in Figure 53 we can see where the largest current spikes occur. The voltage of the battery keeps a steady charge for around 3000 seconds before ultimately showing a downtrend. As 4.191 kW-Hours are pulled out of the system, 2.854 kW-hours are added back into the system through solar charging.

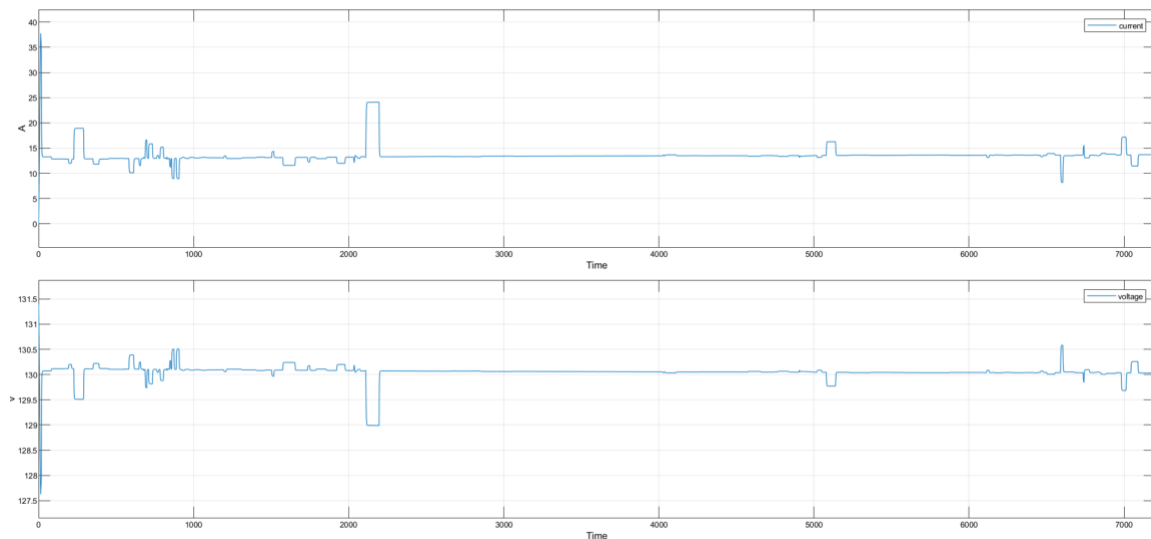


FIGURE 53: Battery Current and Voltage Uphill

The third simulation was conducted using the same parameters as the second simulation except the grade data from UNCC to Appalachian was reversed to test how the system reacts to downhill motion. Figure 54 describes the battery and vehicle characteristics of downhill motion. As expected there are significant differences between the two charts. The overall PG dipped toward the negative range indicating a track in downward motion. The overall velocity didn't stray too far from the other graph which was expected, but during periods of significant downward slope, the velocity exceeded the setpoint. This is due to gravity being sufficient to accelerate the vehicle down the slope, without any input of the motor. The model does not include the impact of braking and as such, the speed controller never provides a negative or braking torque, allowing the velocity to exceed the setpoint.

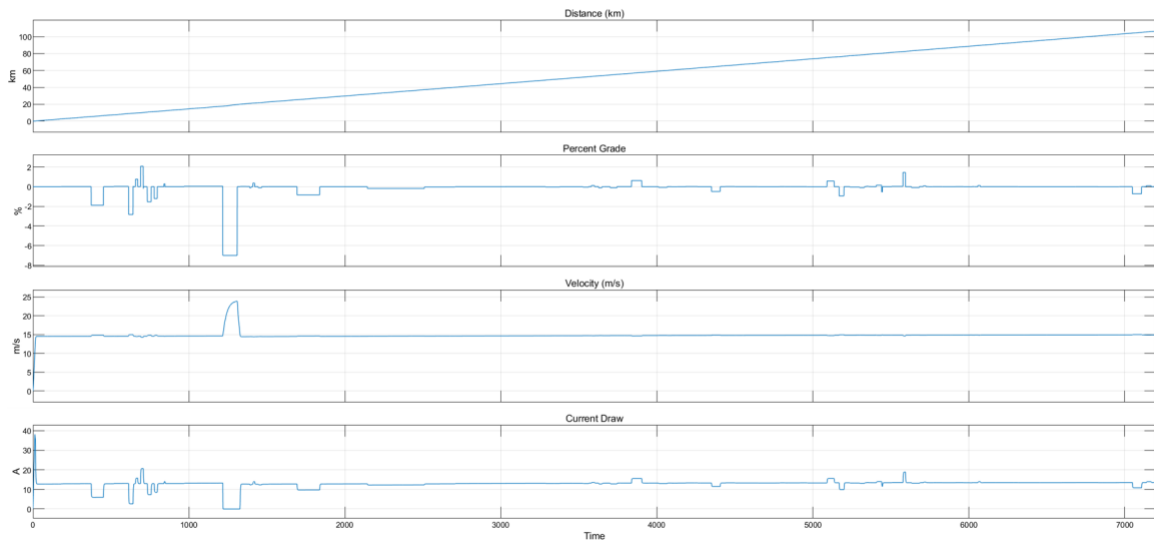


FIGURE 54: Battery and Vehicle Characteristics Downhill

Figure 55 shows the voltage and current results from the battery during the reverse track simulation. The current model is the same as discussed in Figure 52 but in reverse. The voltage has some interesting differences from the first simulation. The current drop around the 1000 second mark shows a drastic decrease in elevation; this sudden drop in current allows the voltage to return to 131 V for a short period, as the lack of load on the battery reduces the drop due to internal resistance. As the model progresses, the sudden change in elevation decreases which is displayed in the graph as the yellow line evens out over time. A downhill climb can become a great asset to solar EV racing when regenerative braking is attached. The data from the graph shows that the EV could vastly benefit not only from direct solar output but regenerative braking as well.

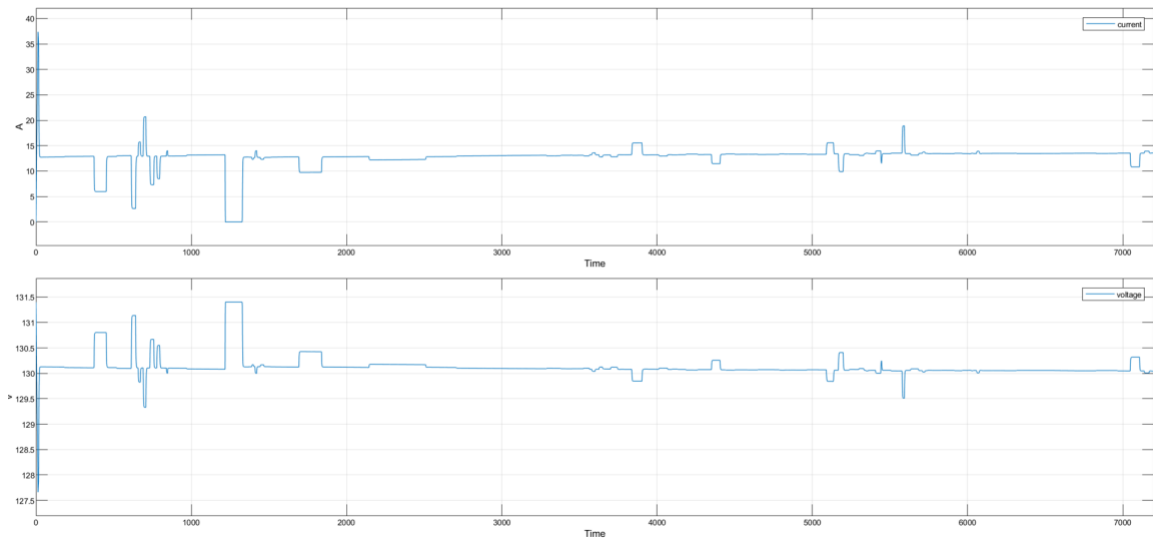


FIGURE 55: Battery Current and Voltage Downhill

To improve upon the system's performance (battery range), increase the amount of solar capacity being used to recharge the battery and utilize regenerative braking to recover energy on the downward slopes. This will redirect that energy back into the system to allow longer travel distances. Some of the grade levels are rather extreme and this data was taken from a third-party application and, therefore, would need to be verified before using it for an actual measurement of performance. Figure 56 and Figure 57 show that the vehicle requires an average of 3.873 kW-hr. The amount of energy that is put back into the system is on average 2.854 kW-hr. This comes directly from the solar cells, which replenish close to 73% of the energy that is being consumed by the motors. These figures are used as an example and do not constitute real world data, the solar panel energy output does not account for electrical losses in charging the battery or changing weather conditions. The data is also pulled from simulation three where a lot of the traveling was downhill which results in less current draw.

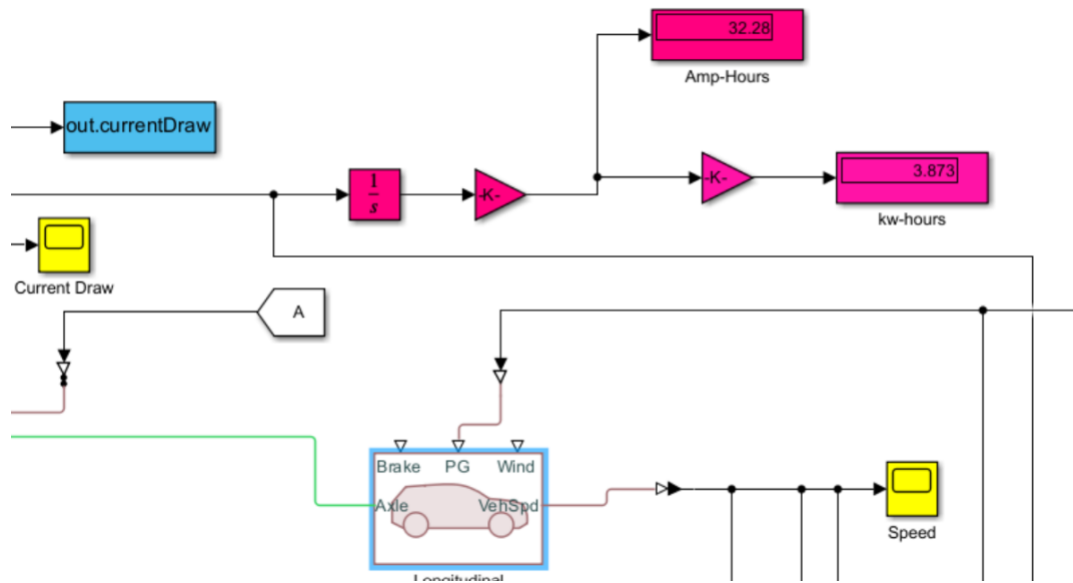


FIGURE 56: Energy Taken from Vehicle Model

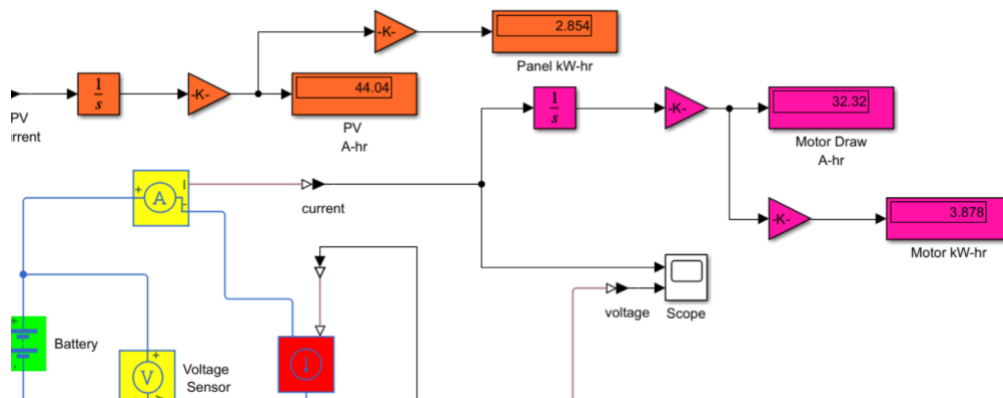


FIGURE 57: Energy Added from Solar Cells

While the models presented have shown the ability to model the general behavior of a solar EV, there are limitations to this model that would require more complex coding to achieve a more refined model of a solar EV system. Mechanically, the model does not represent stop lights or stop signs, so the vehicle remains at a constant velocity the entire trip. The model does not represent regenerative braking; it could provide tremendous benefits by adding energy back into the system. The control of the car does not represent a driver, but instead, a PI controller that simulates a constant speed of 15 m/s. Electrically, solar cells have limited data and would need further refinement of the exact type of cell and its characteristics. No thermal or weather conditions are present during solar recharging; this simulation is based on consistent energy flow into the solar cell. The battery is limited in its parameter data set and further battery information was not included in the model- only the overall characteristics of the battery were included.

Figure 58 is a graphic displaying the model limitations.

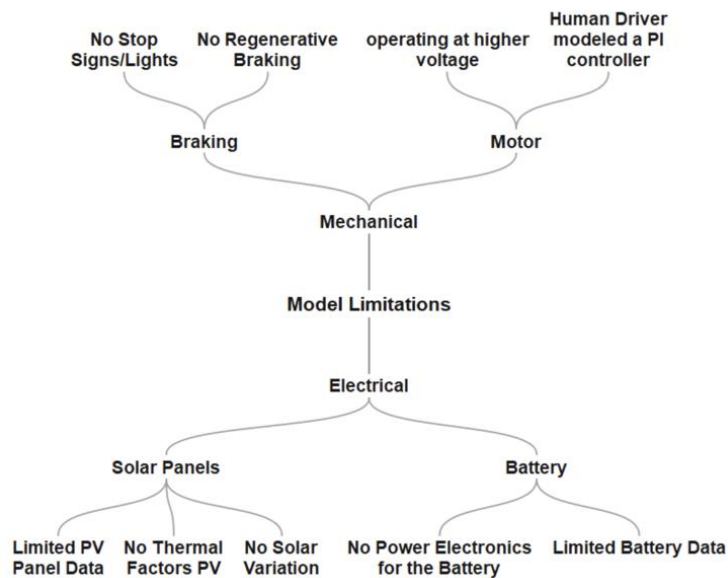


FIGURE 58: Model Limitations

CHAPTER 6: CONCLUSIONS AND FUTURE WORK

The purpose of this research was to develop and utilize DT technology for a solar powered race car built by Appalachian State University called ROSE. A digital twin was created using Simscape software that can benefit the progression of solar EV racing. Digital twin technology can shape the solar racing EV industry's future by digitizing physical assets to efficiently study their behavior. As history has shown, there has long been an interest in EV development, and that interest has grown tremendously in recent years. As interest grows, so does the technology and the need for DTs. DT technology can model real-life objects, which allows for a better understanding of the object's physical nature.

ROSE was modeled as a DT in order to predict the 1-D elements of the vehicle's outputs on a track environment. The methodology used in converting ROSE into a DT used Simscape to model the vehicle dynamics, the battery system, and the solar cell system. The results of the simulation include the vehicle's local position, characteristics of the battery, and solar cell characteristics. The simulation of ROSE as a DT shines light on the basic functionality of how a solar EV responds to different track terrains but requires a deeper level of modular coding to represent the full potential of ROSE.

The DT model needed to encompass as much of the vehicle as possible including mechanical and electrical domains. Using Simscape, a digital model was created that represents all of the main subcomponents of ROSE. The motor was modeled and simulated to mirror the exact outputs that were present in ROSE. The battery and electrical subsystem were modeled using data provided by Appalachian State. The electrical data, such as nominal voltage and cell capacity, were gathered from the actual

characteristics of the battery used in ROSE. The mechanical section of the vehicle modeled the vehicle dynamics of ROSE; this included the weight, drag force, and tire characteristics of the vehicle. The results of the digital model indicate that the software Simscape is easily capable of converting the physical domain into digital domain. The model was successful in converting all necessary components into a digital representation of the solar vehicle as a whole.

A comprehensive simulation of a solar race vehicle must extend beyond the vehicle itself and include the race course. A flat track and incline track were necessary in order to simulate the differences between SOC rates of the battery when grade was present. To simulate a graded track, a function was created that imported data, such as distance and elevation, into a lookup table. An initialization function was responsible for parsing input data, such as current vehicle location versus track distance and elevation, and saving it as the lookup table. The output was the grade value needed to simulate elevation changes. The model was designed to allow custom track data to be imported into the model.

The study required the model to output useful data that could be helpful to a solar EV race team. The outputs of the model represent the energetic state of the battery during track simulation; the model outputs the voltage and current of the battery based on vehicle positioning along the road course. The road course factored in grade changes that directly influence the battery's voltage, current, and SOC levels. The research also required outputs on the energy going into the system via solar cells and energy taken out of the system via the electric motors. Considering that the parameters of the solar cell characteristics can be modified to match a wide variety of panel types and layouts, a

simple block in Simscape was used to represent multiple variations of solar cells. The parameter functionality gives the option to pick specific types of solar cell manufacturers from a comprehensive list. Depending on the settings used for the solar cell, the model pulls direct data from the solar cell block and displays the energy produced by the solar cell system in kW-hrs. The same data is taken from the current draw of the two electric motors and the energy spent is displayed in kW-hrs. The display blocks are beneficial for quick analysis of data that is captured from the inputs of the model's simulation.

The goal was to produce a model that was efficient at generating helpful information, but it was imperative that the model was simple, easy to understand, and quick at solving the calculations. The reason that Simscape was chosen over other software options was the fact that block style coding is great at visualizing the flow of energy and information in the model. As important as the readability, Simscape natively allows for modeling of multiple physical domains (electrical, mechanical, etc.) and supports the conversion between those domains with standard blocks. Each block can have multiple use case factors that can be changed or modified in one single parameter section, which saves time in the field when testing different scenarios. The block layout style of programming is also easy to navigate the attachments of surrounding elements. For the vehicle and solar/battery model, it is easy to see all the subcomponents of the model on one screen, which allows for easy connection style inputs and outputs that improve model creation time.

There are limitations present within the model that allow for growth in future research and development of the digital twin. The digital twin is modeled at the system level and does not have all of the details of a component level model included (motor

controllers, power electronics, wiring losses, etc.). The track simulation of the model is limited by the accuracy of the data taken from the third-party website, Brouter (a bicycle route planner). The data that the track simulation used was solely used to display the functionality of the model's ability to produce PG variables from raw data; however, it was not confirmed as an accurate depiction of elevation change on the route from UNCC to Appalachian State. There is nothing unique about the data produced by the Brouter that is required for the DT. Any CSV data set that includes course length and elevation can be imported into the model. The ability to produce accurate grade results will depend on the precision of distance and elevation data sets obtained.

This research demonstrated the potential for a DT to model the key parameters of a solar electric racing vehicle, but by no means represents the endpoint of integrating a DT into solar racing development. The modular nature of the model lends itself to piecewise refinement of individual aspects of the model as new information becomes available about the subsystems or operational scenarios. Specific improvements could take place in the vehicle model, solar/battery model, and the modeling on the course.

Vehicle model improvements could include higher fidelity component models and validation of component models against actual hardware. Examples of higher fidelity component models include motor controller electronics and the thermal modeling of the motor. Thermal loads could impact motor performance and would be an important factor to include for simulated races in hot climates. Both existing models and higher fidelity models would benefit from benchtop testing (dynamometer) that can verify the performance specifications, ensuring that the models represent actual specifications not just published specifications. A key mechanical interaction that was not modeled in

detail was the tire road interactions. This could be explored and modeled in greater detail and at the very least as parameters that could be changed from course to course and potentially as road conditions that change within a course. Finally, the model could be transitioned from a simple longitudinal model to a multiple degree of freedom model. That would allow for insights into vehicle stability and performance in curved sections of courses, etc. However, that would require a significant investment of time over the existing longitudinal model.

There are opportunities to improve multiple aspects of the solar/battery model. Introduction of the MPPT electronics that govern the charging of the battery would be a step forward in model fidelity as well as more in depth modeling of the battery parameters. The losses from wiring runs and ancillary systems (lights, fans, etc.) are not currently considered in the model but would add to the accuracy of the model. Revisiting the solar panel parameters and updating them to include temperature dependence would augment the veracity of the model. Elevated temperatures are known to degrade solar panel performance, therefore, races in extreme environments should have temperature factored into the simulations.

Finally, the course itself could be augmented to better represent the dynamics of a real race. The introduction of stops or speed changes along the course would be more representative of actual road course driving. Similar to the grade calculations, this could be implanted with a lookup table for planned stops along the route. The environmental conditions could also be simulated to include the ambient temperature, which would impact the motors and electronics as previously mentioned, but more importantly, the solar irradiance could be varied to represent changes in irradiance throughout the day or

the impact of cloud cover during a particular leg of the race. Given a reliable weather forecast for the race the following day, information from these simulated weather conditions could impact driving strategy (speeds, stops, etc.) for optimum performance.

The development of a DT for a solar powered electric race vehicle will dispel solar race EV performance-based questions. The software is dynamic and fast at executing different simulations that require deeper analysis for upcoming solar EV races. The DT model can add a competitive advantage by displaying the strengths and weaknesses of the DT that is modeled. The customizability of the model will also allow new variations of the DT to be uploaded with ease.

The ability to model and replicate a physical object or system in order to predict its behavior is a powerful tool to have in data analytics. The benefit of having a physical object represented as a DT is the ability to have a functioning working model that tracks changes from the physical vehicle. This working model, along with other simulated external environments, can be utilized in competitive solar EV racing. The direct outputs of this model can influence important EV decisions that can aid in competitive racing environments. The model contains important characteristics that help the end user identify the amount of energy entering and exiting the system. The model displays the energy going into the system through the data retrieved from the solar cell subsystem. The energy going out of the system is captured from the motor and the battery. The energy taken out of the vehicle is represented by voltage, current draw, and SOC. All outputs are also directly related to track elevation changes. These changes are tracked as a function of time and can be customized for any track environment. This model will benefit the end user by capturing the digital essence of a physical EV. The model can

easily adapt to all future design changes to ROSE; this in turn will reduce the amount of software simulations needed in order to model the DT. The software is designed to grow with the solar EV; as the EV changes so does the model. The adaptability, ease of programming, and quick processing time makes this DT model a critical asset within the solar racing community.

REFERENCES

- [1] Matulka, R. *The History of the Electric Car*. 2014; Available from: <https://www.energy.gov/articles/history-electric-car>.
- [2] Gross, T. *Technology Snapshot*. Available from: https://afdc.energy.gov/files/pdfs/insight_snapshot.pdf.
- [3] Erik Gregersen, B.A.S. *Tesla Inc*. 2023.
- [4] Sage, E. *How Long Does it Take to Charge Your Tesla?* 2022; Available from: [https://www.energysage.com/electric-vehicles/charging-your-ev/charging-a-tesla/#:~:text=The%20NEMA%2014%2D50%20charger,\(for%20the%20Model%20X\)](https://www.energysage.com/electric-vehicles/charging-your-ev/charging-a-tesla/#:~:text=The%20NEMA%2014%2D50%20charger,(for%20the%20Model%20X)).
- [5] Korosec, K. *Tesla's New V3 Supercharger Can Charge up to 1,500 Electric Vehicles a Day*. 2019; Available from: https://techcrunch.com/2019/07/18/teslas-new-v3-supercharger-can-charge-up-to-1500-electric-vehicles-a-day/?guccounter=1&guce_referrer=aHR0cHM6Ly93d3cuZ29vZ2xlLmNvbS8&guc_referrer_sig=AQAAAE_SifJb2z6SqCIXxE7rJrOgWirAlbIgXRK_nybq9vo0vBDDLgwCVbba_b2rZ0WjDNIZmXde52hRrIgbC6GXxk1KFtsDIx1_XZvXpLrwxZDFSSCt2UodCGmyEMBkewQVcw5rWs5bZc7VpRoIAO-90G1-uwci0eUbU3T2q0eGfZ-c.
- [6] Sahoo, A., S. Sahithi, and J. Channegowda. *Improved Electric Vehicle Digital Twin Performance Incorporating Detailed Lithium-ion Battery Model*. in 2022 *IEEE International Conference on Electronics, Computing and Communication Technologies (CONECCT)*. 2022.
- [7] Slough, J., et al. *Modeling and Simulation of Electric Vehicles Using Simulink and Simscape*. in 2021 *IEEE 94th Vehicular Technology Conference (VTC2021-Fall)*. 2021.
- [8] Hyde, R.A. *Using Simscape™ to support system-level design*. in *UKACC International Conference on Control 2010*. 2010.
- [9] Yaïci, W., et al. *Dynamic Simulation of Battery/Supercapacitor Hybrid Energy Storage System for the Electric Vehicles*. in 2019 *8th International Conference on Renewable Energy Research and Applications (ICRERA)*. 2019.
- [10] Cobbenhagen, R., *Performance analysis of solar cars for everyday use*. 2016.
- [11] Press, K. *The Ugly Duckling*. 1976; Available from: <https://www.alamy.com/oct-18-1976-the-ugly-duckling-makes-its-debut-the-worlds-first-civilian-image69486820.html>.
- [12] MathWorks. *Solar Example*. 2023; Available from: <https://www.mathworks.com/matlabcentral/mlc-downloads/downloads/d589ebaf-1a4b-4fa4-9278-b2ca3ac9ffd4/5c1904af-2394-4bf4-b7ab-082db55c838b/images/screenshot.jpg>.
- [13] Marks, L. *History of Solar Car Racing and the Solar Car Challenge*. 1995; Available from: <https://www.solarcarchallenge.org/challenge/history.shtml>.

- [14] Knight, M. *Solar-powered car smashes speed record*. 2011; Available from: <http://edition.cnn.com/2011/TECH/innovation/01/10/solar.car.world.record/index.html>.
- [15] Garluna, J. *Measuring Solar Cell Efficiency: A Comparative Study of Energy Conversion Efficiency of Solar Cells of the Solar Electric Vehicle, STC-3 at the World Solar Challenge in Australia and at Test Drives on Sathorn Road in Bangkok, Thailand*. in *TENCON 2022 - 2022 IEEE Region 10 Conference (TENCON)*. 2022.
- [16] Autodesk. *Digital Architecture*. 2023; Available from: <https://www.autodesk.com/solutions/digital-twin/architecture-engineering-construction>.
- [17] Saracco, R. *Digital Twins: where we are where we go*. 2019; Available from: <https://cmte.ieee.org/futuredirections/2019/07/05/digital-twins-where-we-are-where-we-go-v/>.
- [18] Molitch-Hou, M. *Virtual Cities to Aid in Managing Increasingly Complex Urban Landscapes*. 2017; Available from: <https://www.engineering.com/story/virtual-cities-to-aid-in-managing-increasingly-complex-urban-landscapes>.
- [19] Ibrahim, M., et al. *Overview on Digital Twin for Autonomous Electrical Vehicles Propulsion Drive System*. *Sustainability*, 2022. **14**, DOI: 10.3390/su14020601.
- [20] Shoukat, M.U., et al. *Application of Digital Twin in Smart Battery Electric Vehicle: Industry 4.0*. in *2022 International Conference on IT and Industrial Technologies (ICIT)*. 2022.
- [21] Bai, L., et al. *Digital Twin Modeling of a Solar Car Based on the Hybrid Model Method with Data-Driven and Mechanistic*. *Applied Sciences*, 2021. **11**, DOI: 10.3390/app11146399.
- [22] Stabile, P., et al. *Eco-Driving Strategy Implementation for Ultra-Efficient Lightweight Electric Vehicles in Realistic Driving Scenarios*. *Energies*, 2023. **16**, DOI: 10.3390/en16031394.

APPENDICES

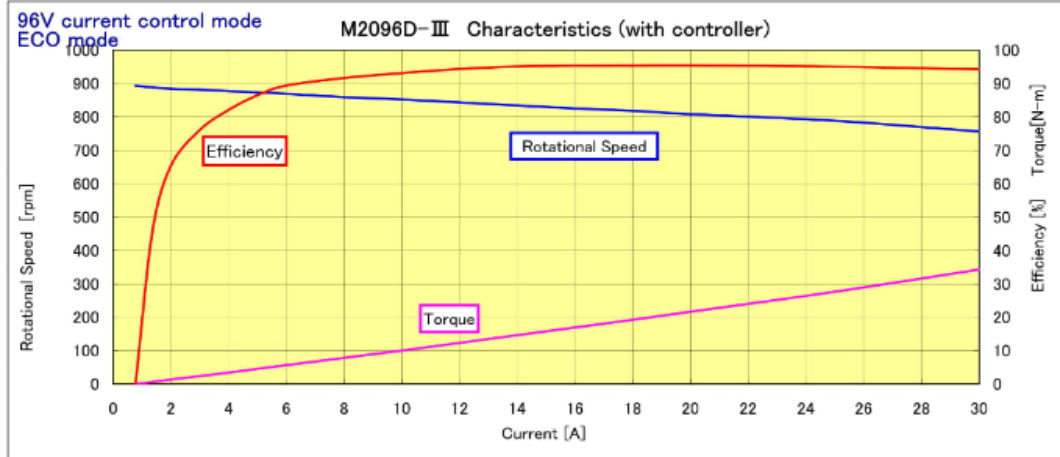
Appendix A: Motor Data Sheet

M2096D-III May-17

current control mode

ECO mode

	MITCHELIN16	93.8	93.2	92.8	92.5	92.1	91.7	91.2	90.2	89.5	88.5	87.6	86.6	85.9	84.8	82.7	79.4 km/h
Current	I(A)	0.780	1.37	2	3	4	5	6	8	10	12	14	16	18	20	25	30
Rotational Speed	N(rpm)	893	888	884	881	877	873	869	859	852	843	834	825	818	808	788	756
Torque	T(kgcm)	0	6.60	13.80	24.20	35.00	46.30	57.70	79.80	102.20	125.60	149.30	172.80	196.20	220.80	282.00	349.70
Torque	T(N·m)	0	0.6	1.4	2.4	3.4	4.5	5.7	7.8	10.0	12.3	14.6	16.9	19.2	21.6	27.6	34.3
Power	(W)	0	60	125	219	315	415	515	703	894	1086	1278	1463	1647	1831	2280	2713
Efficiency	(%)	0	45.7	65.2	76.0	82.0	86.4	89.3	91.6	93.1	94.3	95.1	95.2	95.3	95.3	95.0	94.2



Appendix B: Motor Specifications

Specification item	96V specification
◀Motor▶	
Model	M2096D-III
External dimensions	φ262mm × L59mm
weight	11kg
format	DC brushless motor in-wheel DD
Rated output	2000W
Maximum output	About 5000W*
highest efficiency	95% or more
Rated load speed	810rpm
Direction of rotation	Forward: CCW (counterclockwise) viewed from the wheel mounting surface

Appendix C: Solar Cell Specifications

Solar Cell		<input checked="" type="checkbox"/> Auto Apply ?	
Settings	Description		
NAME	VALUE		
Modeling option	No thermal port ▼		
Selected part	<click to select>		
▼ Cell Characteristics			
Parameterize by	By s/c current and o/c voltage, 5 parameter ▼		
Short-circuit current, I _{sc}	7.34/2	A	▼
Open-circuit voltage, V _{oc}	0.6	V	▼
> Irradiance used for measurements, I _{r0}	1000	W/m ²	▼
Quality factor, N	1.5		
Series resistance, R _s	0	Ohm	▼
▼ Panel Configuration			
Number of series-connected cells per st...	108*2		
Number of parallel-connected strings	3		
> Temperature Dependence			

Appendix D: Battery Specifications

Battery		<input checked="" type="checkbox"/> Auto Apply	?
Settings	Description		
NAME	VALUE		
Modeling option	Instrumented No thermal port		
▼ Main			
> Nominal voltage, Vnom	131.4	V	▼
Current directionality	Disabled		
> Internal resistance	2	Ohm	▼
Battery charge capacity	Finite		
> Cell capacity (Ah rating)	22190/131	A*hr	▼
> Voltage V1 when charge is AH1	127	V	▼
> Charge AH1 when no-load voltage is V1	0.5*22190/131	A*hr	▼
Self-discharge	Disabled		
> Dynamics			
> Fade			
> Calendar Aging			
> Initial Targets			
> Nominal Values			

Appendix E: Motor & Drive Specifications

Motor & Drive		<input checked="" type="checkbox"/> Auto Apply ?	
Settings	Description		
NAME	VALUE		
Parameters			
> Maximum torque	max_torq	N*m	▼
> Maximum power	max_power	W	▼
> Torque control time constant, Tc	Tc	s	▼
> Motor and driver overall efficiency (perc...	motor_eff		
> Speed at which efficiency is measured	speed_eff	rpm	▼
> Torque at which efficiency is measured	torq_eff	N*m	▼
Thermal port	Omit		

Appendix F: Initialization Functions

Model initialization function:

```
1  % PID CONTROL VALUES %
2
3  KP=8; % proportional
4  KI=0.2; % integral
5
6  % PERCENT GRADE DATA %
7
8  %dist=[0 1000 2000 3000 4000 7000 9000];
9
10 %grade=[0 0 1 1.5 0.5 0 0.5];
11
12 %dist=ele(:,1)';
13 %grade=ele(:,2)';
14
15 % VEHICLE MODEL PROPERTIES %
16
17 v_mass=500; % kg
18 tire_radius=0.4064; % m
19 tire_coef=.0136; %
20 drag_coef=0.31; %
21 vehicle_area=2.3; % m^2
22
23 % MOTOR & DRIVE %
24
25 max_torq=68.6; % N*m
26 max_power=3662; % W
27 Tc=0.02; % s
28 motor_eff=95.3; %
29 speed_eff=3750; % rpm
30 torq_eff=100; % N*m
```

```
% PID CONTROL VALUES %
setSpeed=15; % m/s
KP=40; % proportional
KI=0.0125; % integral

% PERCENT GRADE DATA %

dist=[0 1000 2000 3000 4000 7000 9000];
%dist=[0 1 2 2.5 3 3.25 4 5 6];
%dist=15000*dist;

grade=[0 0.5 2.5 3 1.75 1 0.5 1.5 0.5];

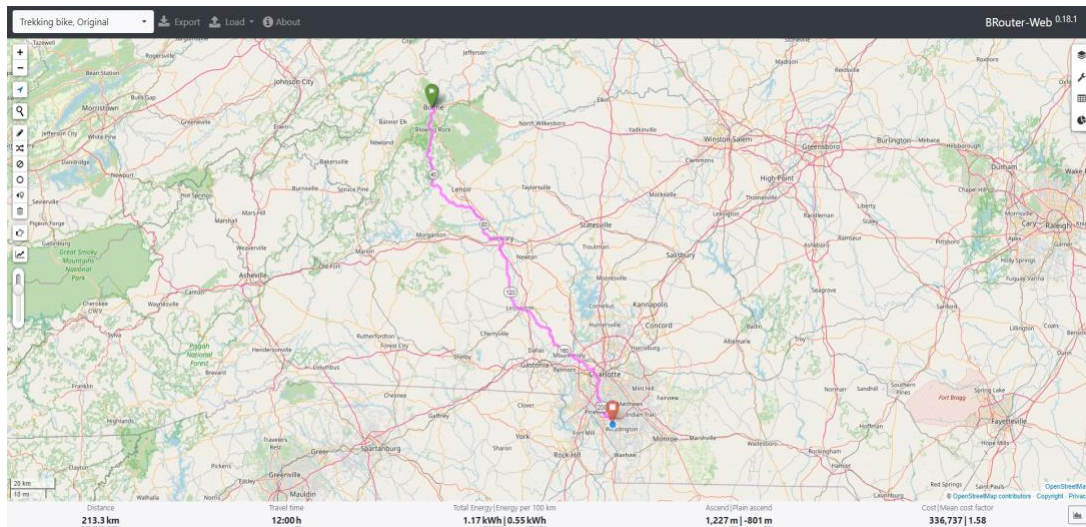
%grade=ones(1,9)*(3);
dist=ele(:,1)';
grade=ele(:,2)';

% VEHICLE MODEL PROPERTIES %

% v_mass=500; % kg
v_mass=300; % kg
tire_radius=0.2; % m
tire_coef=.0136; %
drag_coef=0.31; %
vehicle_area=2.3; % m^2

% MOTOR & DRIVE %
mVolts=120; % motor voltage (V)
max_torq=68.6; % N*m
max_power=3662; % W
Tc=0.02; % s
motor_eff=95.3; %
speed_eff=3750; % rpm
torq_eff=100; % N*m
```

Appendix G: Elevation & Distance Mapping Software



Appendix H: Distance & Grade Raw Data

The raw data is separated into two columns; the first column is the distance measured in meters. Each distance corresponds to the second column which is the grade level.

12784	-0.09091
12793	-1.11111
13289	0
13329	0.05
13747	-0.00239
13787	-0.025
13857	-0.01429
14121	0.034091
14801	0.005882
15302	0.031936
15945	0.010886
16891	0.005285
17234	0
17302	0.102941
17662	-0.03611
20190	-0.00198
20464	0.025547
21798	0
21813	0.333333
22197	0
22255	0
22546	-0.00344
22827	-0.00356
22870	-0.4186
25148	-0.00088
25195	0
25215	-0.25
25612	0.005038
25969	0
26026	-0.07018
27924	0.000527
28020	-0.32292
29500	0
29596	-0.03125
29599	-0.33333
29702	0.087379
29905	0
29998	-0.06452
30401	0.024814
30744	0
30752	2.875
33180	0.006178
36596	0.009368
40714	-0.00024
40860	-0.00685
42416	0.012853
47097	0.003204

57383	0.000972
59012	0.000614
59074	0.048387
59248	-0.00575
59303	0.054545
61362	0.005828
63672	-0.00043
67039	-0.00149
67378	-0.03245
69467	0
69867	-0.01
70339	-0.04449
71886	-0.00194
72118	-0.00431
72133	-0.13333
72202	0
72228	-0.03846
72942	-0.02521
73418	-0.0084
73807	0.002571
73855	-0.10417
74720	0
74767	0.723404
76501	-0.00115
77267	0.016971
80593	0.001804
81513	0.007609
83244	0.012132
89862	-0.0003
89997	0.014815
90120	0
90153	-0.12121
90601	0.004464
90840	-0.00837
91004	0.018293
91328	0.009259
91610	0.010638
91920	-0.00968
93106	0.006745
94427	0
94923	0.008065
95243	-0.0125
95411	-0.08333
95738	-0.01223
96140	0.08209
97267	0
97273	0

97284	-1.45455
97717	-0.03233
99450	0.000577
99463	0.538462
99602	-0.15108
100478	-0.00342
100619	-0.01418
100910	-0.03436
101078	0
101250	0.087209
102027	0.039897
103112	0
103127	0.933333
104045	0
104062	-0.58824
105396	0.017991
107858	0.001219
108560	0
108950	-0.00769
109523	0.012216
113065	0.000565
113879	-0.01843
114827	-0.00316
114888	0.491803
116483	0.001881
117539	-0.02083
118717	0.005093
119099	0.015707
119861	0.001312
119889	0.071429
121503	0.006815
121921	0.011962
122136	0.004651
122243	0
122329	-0.62791
124173	-0.00597
124473	-0.01
124757	0.098592
125781	0.001953
125904	0.00813
125973	0.014493
126095	0.106557
126627	-0.0094
126838	-0.11848
127230	-0.01531
127341	0.045045
128332	0.013118

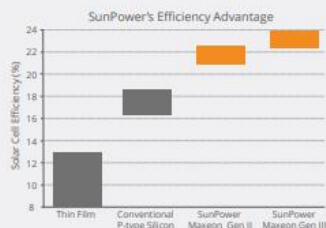
129494	0.007745
130517	0.031281
132171	0.001209
137974	0.005514
141723	0.034409
143736	0.17685
152399	0.002424
152605	0.830097
156677	-0.00909
157914	0
157924	0.1
158556	-0.00316
158586	-0.36667
158882	0.003378
158901	0.105263
159171	-0.01852
159512	-0.02639
160262	-0.00133
160275	7
164251	-0.04477
167551	-0.00091
167608	0
167678	0.014286
167695	-0.29412
167882	0
167884	0
168246	0.002762
168260	0
168383	0
168404	0
168423	1.210526
168979	0
168992	1.538462
169717	0
169722	0.2
169734	-2.08333
170233	-0.002
170250	-0.76471
170659	-0.00244
170678	-0.05263
170690	2.833333
171534	-0.03318
173438	-0.00053
173466	1.892857
175783	-0.0164
179066	0.010661
179917	0.010661

Appendix I: Solar Cell Datasheet

MAXEON™ GEN III SOLAR CELLS

Power Advantage

SunPower designs, manufactures, and delivers high-performance solar electric technology worldwide. SunPower™ cells produce 25-35% more power compared to Conventional Cells¹ with outstanding aesthetics.



Energy Advantage

SunPower panels deliver the highest energy per rated watt compared to a Conventional Panel. (Photon International, Mar 2013, out of 151 panels tested).

- No Light-Induced Degradation = 2 - 3% more energy.
- No Temperature Coefficient = 1 - 2% more energy at 35-40°C ambient temperature.
- Low Light and Broad Spectral Response = up to 1% more energy in overcast and low-light conditions.

¹ As used throughout, "Conventional Cells" are silicon cells that have many thin metal lines on the front and 2 or 3 interconnect ribbons soldered along the front and back. "Conventional Panel" means a panel with 240W, 15% efficiency and approximately 1.6 m² made with Conventional Cells.

Durability Advantage

The Maxeon cell has strength and durability to survive extreme conditions year after year, enabling SunPower to provide superior, long-term performance in a broad range of applications.



- Corrosion Resistance: SunPower's tin-copper metal system is more corrosion resistant compared to the porous metal paste used in Conventional Cells, which can crack more easily and corrode.
- Crack Resistance: SunPower's cells are thinner and more flexible than Conventional Cells. When a SunPower cell does crack, the backside copper metal foundation keeps the cell intact and maintains a high power output. When Conventional Cells crack, the cell breaks apart with typically a significant loss of power.
- Eco-Friendly: SunPower cells solder to lead-free components and are RoHS compliant. Conventional Cells often require components with lead.

MAXEON™ GEN III SOLAR CELLS

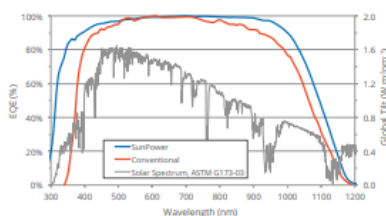
Electrical Characteristics of a typical Maxeon Gen III Cell At Standard Test Conditions (STC) STC: 1000W/m², AM 1.5G and cell temp 25°C

	Cell Bin	P _{mpp} (Wp)	Eff. (%)	V _{mpp} (V)	I _{mpp} (A)	V _{oc} (V)	I _{sc} (A)
Ultra Peak Performance	Me1	3.72	24.3	0.632	5.89	0.730	6.18
Ultra Premium Performance	Le1	3.63	23.7	0.621	5.84	0.721	6.15
Ultra High Performance	Ke1	3.54	23.1	0.612	5.79	0.713	6.11

Electrical parameters are nominal values.

Temp. Coefficients in SunPower Panels: Voltage: -1.74mV/°C, Current: 2.9mA/°C, Power: -0.29%/°C

Spectral Response



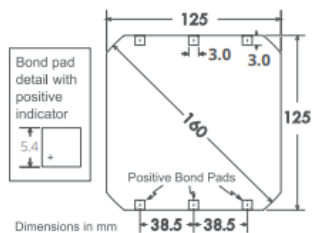
References

SunPower: NREL data, commissioned by SPWR

Conventional: Progress in Photovoltaics: Research and Applications, Solar cell efficiency tables, version 36 18(5), (2010) 46-352

Cell Physical Characteristics

Wafer:	Monocrystalline silicon
Design:	All back contact
Front:	Uniform, black antireflection coating
Back:	Tin-coated, copper metal grid
Cell Area:	Approximately 153cm ²
Cell Weight:	Approximately 6.5grams
Cell Thickness:	150µm +/- 30µm



Bond pad area dimensions are 5.4mm x 3.0mm
Metal finger pitch between positive and negative fingers is 471µm.
Positive/Negative pole bond pad sides have "+/-" indicators on leftmost and rightmost bond pads

Positive Electrical Grounding

If cell voltage is below frame ground the cell power output will be reduced. Therefore, modules and systems produced using these cells should be configured as "positive ground systems." If this creates a problem, please consult with SunPower.

Interconnect Tab and Process Recommendations



SunPower recommends customers use SunPower's patented tin-plated copper strain-relieved interconnect tabs, which can be purchased from SunPower. These interconnects are easily solderable and compatible with lead free processing. Tabs weigh approximately 0.3 grams.

Our patented interconnect tabs are packaged in boxes of 3600 or 36,000 each.

<http://us.sunpower.com/about/sunpower-technology/patents/>

Production Quality

ISO 9001:2015 certified

Soft handling procedures to reduce breakage and crack formation

100% cell performance testing and visual inspection

Packaging

Cells are packed in boxes of 1500 each; grouped in 10 shrink-wrapped stacks of 150 with interleaving, 24 boxes are packed in a water-resistant "Master Carton" containing 36,000 cells suitable for air transport.

Purchase Terms

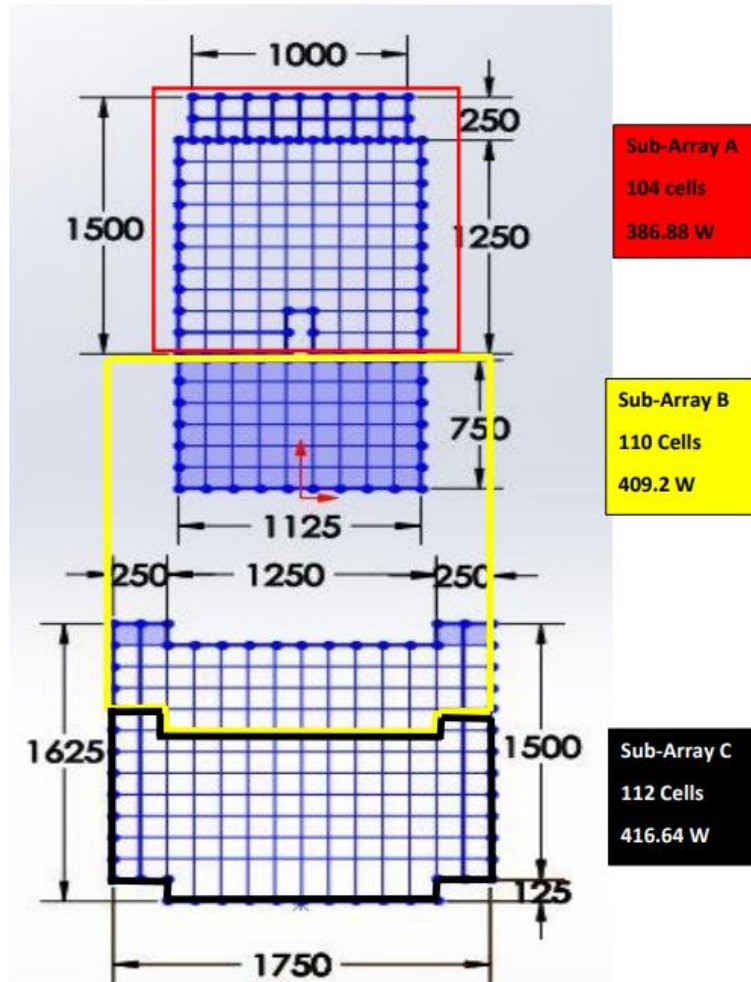
Customers shall not reverse engineer, disassemble or analyze the Solar Cells or any prototype, process, product, or other item that embodies Confidential Information of SunPower. Customers shall not cause or allow any inspection, analysis, or characterization of any properties (whether mechanical, structural, chemical, electrical, or otherwise) of the Solar Cells, whether by itself or by a third party.

Customer agrees that it will not transfer (whether by sale, loan, gift, or other conveyance) the Solar Cells from its possession.

SunPower solar cells are provided "AS IS" without warranty.

Full terms and conditions are in the Cell Purchase Agreement

Appendix J: Solar Array Data



Total power: $386.88\text{W} + 409.2\text{W} + 416.64\text{W} = 1,212.72\text{W}$
 Total cells: $104\text{ cells} + 110\text{ cells} + 112\text{ cells} = 326\text{ cells}$
 Photovoltaic surface area: $326\text{ cells} \times 153.33\text{ cm}^2 = 49985.58\text{ cm}^2 = 4.999\text{ m}^2$

Appendix K: Solar Vehicle Energy Balance

$$v = 15 \left[\frac{m}{s} \right]$$

$$t = 2 [hr]$$

$$dist = v \cdot t = 108000 [m]$$

$$aDen = 1.3 \left[\frac{kg}{m^3} \right]$$

$$area = 2 [m] \cdot 1 [m] = 2 [m^2]$$

$$Cd = 0.21$$

$$Fd = 0.5 \cdot Cd \cdot area \cdot aDen \cdot v^2 = 61.425 [N]$$

$$dragWork = Fd \cdot dist = [MJ] = 6.6339 [MJ]$$

$$mass = 300 [kg]$$

$$g = 9.8 \left[\frac{m}{s^2} \right]$$

$$h = 530 [m]$$

$$PE = mass \cdot g \cdot h = [MJ] = 1.5582 [MJ]$$

$$flatEnergy = 34.66 [A \cdot hr] \cdot 120 [V] = [MJ] = 14.97312 [MJ]$$